

2001-04

# Thalamocortical dynamics of the Mccollough Effect: boundary-surface alignment through perceptual learning

---

<https://hdl.handle.net/2144/2280>

*"Downloaded from OpenBU. Boston University's institutional repository."*

**Thalamocortical dynamics of the McCollough  
Effect: Boundary-surface alignment through  
perceptual learning**

Stephen Grossberg, Seungwoo Hwang and Ennio Mingolla

**April, 2001**

**Technical Report CAS/CNS-01-004**

Permission to copy without fee all or part of this material is granted provided that: 1. The copies are not made or distributed for direct commercial advantage; 2. the report title, author, document number, and release date appear, and notice is given that copying is by permission of the BOSTON UNIVERSITY CENTER FOR ADAPTIVE SYSTEMS AND DEPARTMENT OF COGNITIVE AND NEURAL SYSTEMS. To copy otherwise, or to republish, requires a fee and / or special permission.

Copyright © 2001

Boston University Center for Adaptive Systems and  
Department of Cognitive and Neural Systems  
677 Beacon Street  
Boston, MA 02215

# THALAMOCORTICAL DYNAMICS OF THE McCOLLOUGH EFFECT: BOUNDARY-SURFACE ALIGNMENT THROUGH PERCEPTUAL LEARNING

Stephen Grossberg\*, Seungwoo Hwang<sup>†</sup> and Ennio Mingolla<sup>‡</sup>

Department of Cognitive and Neural Systems  
and Center for Adaptive Systems  
Boston University

April, 2001

Submitted to *Vision Research*

**Technical Report CAS/CNS TR-01-004**

*All correspondence should be addressed to:*

Professor Stephen Grossberg  
Department of Cognitive and Neural Systems  
Boston University  
677 Beacon Street  
Boston, MA 02215  
Phone: 617-353-7858  
Fax: 617-353-7755  
Email: [steve@cns.bu.edu](mailto:steve@cns.bu.edu)

Key words: Color perception, Binocular vision, Perceptual learning, Visual cortex,  
Aftereffects, Boundary segmentation, Surface representation,  
McCollough effect, FACADE model

Running Head: McCollough Effect and Boundary-Surface Alignment

---

\*Supported in part by the Defense Advanced Research Projects Agency and the Office of Naval Research (ONR N00014-95-1-0409) and the Office of Naval Research (ONR N00014-95-1-0657)

<sup>†</sup>Supported in part by the Defense Advanced Research Projects Agency and the Office of Naval Research (ONR N00014-95-1-0409) and the Office of Naval Research (ONR N00014-92-J-1309 and ONR N00014-95-1-0657)

<sup>‡</sup>Supported in part by the Defense Advanced Research Projects Agency and the Office of Naval Research (ONR N00014-95-1-0409)

## Abstract

This article further develops the FACADE neural model of 3-D vision and figure-ground perception to quantitatively explain properties of the McCollough effect. The model proposes that many McCollough effect data result from visual system mechanisms whose primary function is to adaptively align, through learning, boundary and surface representations that are positionally shifted, due to the process of binocular fusion. For example, binocular boundary representations are shifted by binocular fusion relative to monocular surface representations, yet the boundaries must become positionally aligned with the surfaces to control binocular surface capture and filling-in. The model also implicates perceptual reset mechanisms that use habituating transmitters in opponent processing circuits. Thus the model shows how McCollough effect data may arise from a combination of mechanisms that have a clear functional role in biological vision. Simulation results with a single set of parameters quantitatively fit data from thirteen experiments that probe the nature of achromatic/chromatic and monocular/binocular interactions during induction of the McCollough effect. The model proposes how perceptual learning, opponent processing, and habituation at both monocular and binocular surface representations are involved, including early thalamocortical sites. In particular, it explains the anomalous McCollough effect utilizing these multiple processing sites. Alternative models of the McCollough effect are also summarized and compared with the present model.

## 1 Introduction

A neural model of binocular boundary and surface perception is developed whose adaptive mechanisms can explain a number of key properties of the McCollough effect (ME), including interocular properties which have not previously been explained. The ME (McCollough, 1965) is a complementary color aftereffect, which is typically induced by several minutes of adaptation to gratings of black and color stripes. The ME has many properties that distinguish it from ordinary negative afterimages, including: (1) the ME does not require fixation of adapting stimuli; (2) the ME is orientation-contingent; and, most importantly, (3) the ME can last for hours, days, or even weeks. The ME has attracted much attention because it probes interacting properties of orientational coding, color perception, surface formation, and learning by visual cortex.

McCollough (1965) reported that the ME was monocular, that is, adaptation of only one eye resulted in an effect in the adapted eye but not in the unadapted eye. The absence of interocular transfer of the ME may seem to suggest that binocular loci are not involved in the ME. However, this view has been challenged by subsequent studies which have shown that some interocular properties of the ME do exist, although interocular transfer of the ME does not occur under monocular adaptation.

For example, MacKay and MacKay (1973) found some transfer of visual information between the two eyes. In their experiment, pure orientational information and pure color information was given to each eye separately, such that one eye was adapted to an achromatic grating and the other eye was adapted to a homogeneous colored field. Although neither of the eyes was given an adapting stimulus containing both orientation and color information, a ME was nevertheless induced. Moreover, different aftereffects were obtained for each eye. Testing the color-adapted eye led to a normal aftereffect (that is, the aftereffect exhibits the *complementary* hue to the adapting colored field presented to the same eye), whereas testing the achromatically adapted eye led to an aftereffect that is often referred to as an anomalous ME (that is, the aftereffect exhibits the *same* hue as the adapting colored field presented to the opposite eye). Therefore, in this experiment: (1) orientation transferred interocularly; and (2) color transferred interocularly in such a way that

opposite colors were experienced in the two eyes. MacKay and MacKay (1973) speculated that some kind of interocular transfer of orientation and antagonistic color might have taken place.

Vidyasagar (1976) was probably the first to provide a direct evidence for the idea that binocular neurons are involved in the ME. By using binocular adapting gratings that were made opposite to monocular adapting gratings, both in their orientation and color, it was shown that binocular aftereffects can be made the opposite to monocular aftereffects.

The interocular properties of the ME were further explored in experiments of White *et al.* (1978), where one eye was adapted to a colored grating and the other eye was adapted to a homogeneous colored field. In those experiments, interocular transfer of orientational information occurred when the color of the homogeneous field was made the same as the color of the grating, but not when the color of the homogeneous field was made the opposite to the color of the grating.

There also have been several attempts to provide theoretical explanations of the ME. Several researchers (Shute, 1979; Dodwell & Humphrey, 1990; Warren, 1985; Bedford & Reinke, 1993; Bedford, 1995) have proposed that the ME arises from a process of correcting errors and biases that are imposed during adaptations in ME experiments. Several researchers (Hohmann & von der Malsburg, 1978; Held, 1980; Broerse *et al.*, 1999) proposed that the ME arises from neural mechanisms that compensates for chromatic aberration of the eye. For some researchers (Murch, 1976; Allan & Siegel, 1997), shared features between the ME and Pavlovian conditioning paradigm were viewed as important characteristics of the ME. Still other researchers focused on how the adaptive mechanisms in the nervous system generate relevant changes in neural loci that subserves the ME as their perceptual outcome. Since the ME is contingent on orientation, many researchers have suggested that its locus is in the early stages of cortical processing (see Watanabe *et al.* (1992) for a short review on such neural loci). Some of them suggested that the effect arises from fatigue of neurons that are tuned both to orientation and color (McCollough, 1965; Stromeyer & Dawson, 1978; Michael, 1978). Others suggested that the effect arises from synaptic changes in the connection between neurons for orientation and neurons for color (Murch & Hirsch, 1972; Savoy, 1984; McLoughlin, 1995). Still others suggested that the effect arises from changes within the intrageniculate pathways (Krüger, 1979).

In the aforementioned theoretical studies, however, interocular properties of the ME have rarely been emphasized, with the exception of studies by Savoy (1984) and McLoughlin (1995). Savoy (1984) is probably the first to propose a model of the ME that is aimed at explaining interocular properties of the ME. In his model, the ME is generated by an interaction between an orientation system and a color system. Interocular properties of the ME were achieved by positing that the orientation system is binocular and the color system is monocular. However, since the color system in the model is strictly monocular, the model was not able to explain the anomalous ME data of MacKay and MacKay (1973), where there was an interocular transfer of color information.

Recently, McLoughlin (1995) reported data from a wide range of experimental variations regarding interocular properties of the ME, and replicated the experiments of MacKay and MacKay (1973), Vidyasagar (1976), and White *et al.* (1978), among others. Relative strengths of aftereffects in each experiment were measured in order to collect quantitative data. Then, a neural network model, which resembled the Savoy (1984) model in its overall architecture, was proposed that quantitatively simulated most of these data. Although simulations of the model showed a reasonably good fit to most of the data, the anomalous ME data of MacKay and MacKay (1973) could not be explained by the model, since the model allows only orientational information to be transferred interocularly, but not color information.

The present article presents a model of binocular vision that is capable of explaining and quantitatively simulating all the known key properties of the ME, including the interocular properties. The model further develops a neural network theory of binocular vision called FACADE theory

(Grossberg, 1987, 1994, 1997; Grossberg & McLoughlin, 1997). Indeed, the first article on FACADE theory (Grossberg, 1987) qualitatively explained a number of ME data, including interocular properties, but did no simulations to quantitatively test its validity. A key hypothesis of the Grossberg (1987) model is further developed herein; namely, that the ME arises using visual system mechanisms whose primary functions are to adaptively align boundary and surface representations which are positionally shifted with respect to one another due to the process of binocular fusion and allelotropia, or displacement (von Tschermak-Seysenegg, 1952; Werner, 1937), in the boundary system, but not in the surface system, of the visual cortex (Grossberg, 1987). Thus the Grossberg (1987) proposal replaces an orientation and color system by a boundary and surface system. The properties of these boundary and surface systems have elsewhere been used to explain many other types of perceptual and neurobiological data. Since boundaries are used to form the compartments which surface brightness and color signals fill in, the signals between the boundary and surface systems must be positionally aligned. The FACADE model predicts that the signals between the boundary system and the surface system undergo perceptual learning in order to compensate for their mutual displacement. The model also proposes that such adaptive alignment mechanisms are activated by habituated transmitter gates in chromatic opponent processing circuits. These additional mechanisms assure that percepts are rapidly reset in response to temporally changing scenes (Francis & Grossberg, 1996; Francis *et al.*, 1994). The present article shows how to rigorously incorporate such perceptual learning and habituated mechanisms into FACADE theory. The ME is then induced as an emergent phenomenon of these adaptive alignment and habituated mechanisms. The model's proposal of how this happens provides a functionally meaningful explanation of the ME data as a manifestation of boundary and surface interactions. The present article shows how a quantitative implementation of these FACADE mechanisms, which have not been implemented together before, can quantitatively simulate all the key data.

## 2 Theory

### 2.1 Overview of FACADE theory

FACADE (Form-And-Color-And-DEpth) theory suggests that the brain's representation of a visual scene is generated by interactions between two main subsystems: the Boundary Contour System (BCS), and the Feature Contour System (FCS). The BCS forms binocular boundary segmentations that do not carry any visible signal; they are invisible or amodal. The FCS fills in visible surface properties at spatial locations whose boundaries are determined by the BCS. The BCS models properties of the interblob cortical stream, and the FCS models properties of the blob cortical stream (Grossberg, 1994).

Previous works on FACADE theory have shown how it can explain a variety of visual phenomena that are related to the figure-ground problem (Grossberg, 1987, 1994, 1997; Grossberg & Kelly, 1999; Grossberg & McLoughlin, 1997; Grossberg & Pessoa, 1998; Kelly & Grossberg, 1998). In the present article, FACADE theory is further developed in order to quantitatively model the processing stages that are needed to explain ME data. For simplicity, details of FACADE theory that are not needed for this aim are omitted.

### 2.2 Overview of the present model

Figure 1 provides an overview of the model that is developed in the present article. The processing stages in the model are next described before their functional roles in explaining the ME are summarized.

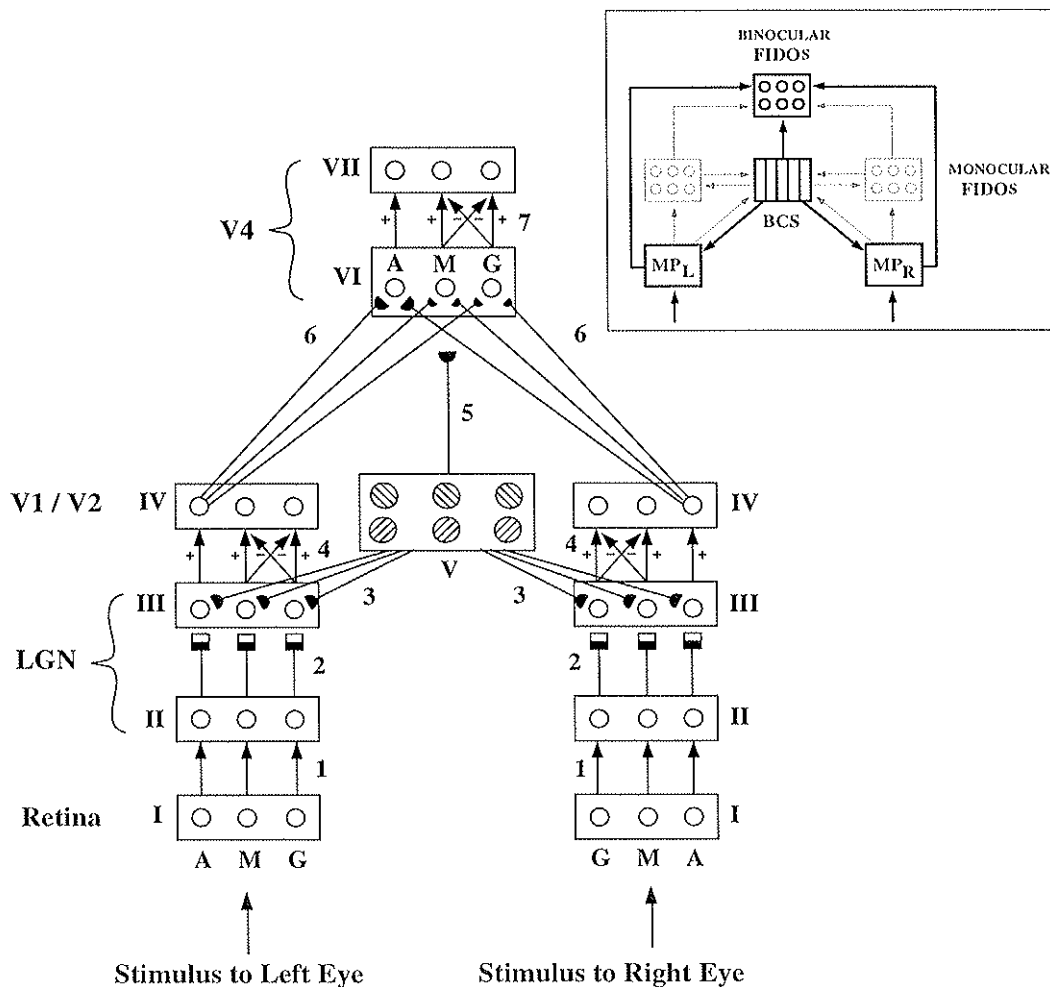


Figure 1: Schematic diagram of the FACADE model used to simulate ME data. Hatched circles denote BCS cells that are tuned to orientation ( $45^\circ$  and  $135^\circ$ ) and to ocularity (left monocular, binocular, and right monocular). Three pairs of open circles denote FCS cells tuned to three colors (achromatic (A), magenta (M), and green (G)). Processing stages in the theory are numbered by Roman numerals. Pathways that connect those processing stages are numbered by Arabic numerals. Pathways that end with hemicircles are gated by adaptive synaptic weights. Pathways that end in black and white squares are gated by habituating or depressing synapses. Pathways that end in arrowheads merely transfer signals from one cell to another. The inset shows a macrocircuit of the FACADE model, including stages and pathways that were implemented in this study (drawn by bold lines), as well as those were not (drawn by thin lines), which are employed in explanations of other phenomena. See text for details.

The first stage (Figure 1, Stage I) of the model consists of three sets of retinal cells that sample the stimulus distribution in each eye. One set of cells (denoted as A in Figure 1) are activated mostly by achromatic stimuli. The other two sets of cells (denoted as M and G in Figure 1) are activated mostly by magenta or green stimuli, respectively.

The cells in the lateral geniculate nucleus (LGN) stage (Figure 1, Stage II and III) receive their inputs from the retinal cells. LGN cells are modeled using feedforward networks with circular concentric on-center off-surround receptive fields that input to cells which obey membrane, or shunting, equations. The properties of these cells, such as discounting the illuminant, contrast normalization, and sensitivity to image reflectances, were discussed in detail by Grossberg (1983)

and used to explain various brightness perception data in Grossberg and Todorović (1988).

Output signals from LGN cells are multiplied, or gated, by habituating or depressing transmitters (Grossberg, 1968, 1969); see Figure 1 (Pathway 2, square synapses). The transmitter habituation is proportional to the strength of the input signal and to the amount of available transmitter. Our model of transmitter habituation is consistent with Abbott *et al.* (1997)'s experimental and modeling work on synaptic depression in cortical cells. Such transmitters play a key role in achieving intracellular adaptation (Carpenter & Grossberg, 1981); rebalancing and resetting neural circuits (Baloch *et al.*, 1999; Francis & Grossberg, 1996; Francis *et al.*, 1994) as well as, in suitable parameter ranges, generating transient neural responses (Baloch *et al.*, 1999; Ögmen & Gagne, 1990). They also play a fundamental role in our ME explanations.

The cells in model areas V1 and V2 of the BCS (Figure 1, Stage V) become active when oriented boundary structures in the stimulus are detected. The BCS contains binocular cells, left monocular cells, and right monocular cells. In this article, the term "binocular cells" refers to cortical cells that are driven equally well by either of the two eyes, and the term "monocular cells" refers to cortical cells that show a strict ocular dominance. Both types of cells are well known to exist (Hubel & Wiesel, 1962). The model does not need to invoke intermediate cell types to simulate ME data. Previous modeling work (Grossberg & McLoughlin, 1997) showed how both types of cells contribute to stereopsis and 3-D boundary and surface perception. The present model further assumes that the binocular cells behave as "OR" gates that respond strongly to binocular stimuli and weakly to monocular stimuli. Some binocular cells *in vivo* have been shown to respond more vigorously to binocular stimulation than to monocular stimulation (Hubel & Wiesel, 1962; Pettigrew *et al.*, 1968). The monocular cells, on the other hand, are assumed to respond strongly to monocular stimuli and weakly to binocular stimuli. Some monocular cells *in vivo* have been shown to respond more vigorously to monocular stimulation than to binocular stimulation (Kato *et al.*, 1981). The relative strengths of binocular and monocular cells under binocular and monocular stimulus presentations are key parameters in the present simulations. The activation of monocular and binocular boundary cells in the model is determined by an algorithm, rather than through network interactions. This was done to simplify our simulations, which focus upon the habituating and learning dynamics of several monocular and binocular processes from LGN through cortical area V4, as in Figure 1. See Appendix for details.

Once activated, these BCS cells send signals along two types of pathways. One of them is a binocular boundary pathway (Figure 1, Pathway 5). It interacts with featural signals to form a visible surface representation by a mechanism of filling-in, as will be described later. The other is a top-down feedback pathway (Figure 1, Pathway 3) from model area V1 to LGN. Consistent with the architecture of the present model, Grieve and Sillito (1995) reported that both the binocular and monocular cells are found in corticogeniculate projecting neurons in layer 6 of the primary visual cortex in cats. Both modeling (Gove *et al.*, 1995; Grossberg *et al.*, 1997) and experimental (Sillito *et al.*, 1994) studies have suggested that the functional role of the corticogeniculate feedback pathway is to select and enhance LGN cell activities that are consistent with cortical cell activities. Other modeling studies (Grunewald & Grossberg, 1998; Grossberg, 1980) further predicted that this feedback pathway possesses adaptive synapses and showed how these adaptive synapses in the feedback pathway undergo experience-dependent learning which helps to stabilize the tuning of binocular disparity in feedforward pathways. A recent study by Murphy *et al.* (1999) showing that these feedback signals to the LGN are spatially distributed with the same orientation as their cortical sources is consistent with the prediction that their synapses can learn.

In addition to these previously suggested functions of the corticogeniculate feedback pathway, the present article shows how this feedback pathway can also contribute to the ME. This is proposed to occur through the modification of its adaptive synapses in response to transmitter habituation in LGN cells that is induced by prolonged viewing of adapting gratings. The learning

in the corticogeniculate feedback pathway is proposed to track postsynaptic cell activity and to be gated by the correlated activities of its presynaptic and postsynaptic cells. As a result, the strength of the pathway changes only when V1 (presynaptic) cells and LGN (postsynaptic) cells are concurrently active. In this manner, the corticogeniculate feedback pathway learns the transmitter-gated LGN cell activities with which the V1 cells are associated. The theory hereby proposes that the effects of this process on the ME are due to the combined effects of the habituation-reset properties of transmitter gates and the stabilizing properties of top-down learning. The proposed learning mechanism in this feedback pathway will be described in detail later in the article. It should also be noted that *any* feedback pathway from the boundary cells to monocular surface representations could play the same role.

The combination of bottom-up transmitter-gated and top-down learned signals, which is realized in the simulations as a multiplication of two signals, is then further transformed by monocular opponent processing (Figure 1, Pathway 4) between magenta cells and green cells to give rise to monocular featural signals (Figure 1, Stage IV). The Stages I through IV comprise the monocular FCS. These monocular featural signals are conveyed by the cortical bottom-up FCS pathway (Figure 1, Pathway 6) to the next stages of surface processing, where the outputs from the monocular FCS are binocularly matched and subsequently filled-in (Figure 1, Stage VI). In the present and previous works on FACADE theory, one function of this pathway was to adaptively align the monocular FCS surface signals with binocular BCS boundaries that are positionally displaced by binocular fusion and allelotropia so that the BCS could control binocular filling-in of 3-D surfaces within the FCS. Grossberg and Kelly (1999) tested the binocular filling-in function by simulating data on binocular brightness perception, including Fechner's Paradox. Here we introduce a learning law into this pathway and show how it can help to explain the ME.

Binocularly summated featural surface properties, such as color, generate a visible surface representation at the final level of the FCS, which is called the Binocular *Filling-In Domain* (FIDO). The binocular FIDO (Figure 1, Stages VI and VII) includes arrays of intimately connected cells such that neighboring cells can rapidly spread activities between each other's compartment membranes. This diffusive spreading, or filling-in, of activation is initiated by binocularly matched featural inputs and is restricted to the compartments that are formed by binocular boundaries (Figure 1, Pathway 5), which act as barriers to filling-in. The net effect of these interactions is that the binocularly summated featural surface properties spread within binocular boundaries. The resultant filled-in activities of magenta and green binocular FIDOs are opponently processed (Figure 1, Pathway 7) to yield a perception of surface color. Together with the cortical bottom-up FCS pathway, the binocular boundary pathway is used to explain the anomalous ME data of MacKay and MacKay (1973), among others.

### 2.3 Qualitative Model Explanation of General ME properties

Core issues in the ME that need to be explained by any theory include why the effect is typically complementary to the adapting color, how the effect becomes long-lasting, and how the effect becomes contingent on orientation. The present theory explains these general properties as follows.

Consider what happens in the network in response to 45° binocular adapting gratings of magenta and black stripes. As shown in Figure 2, prolonged presentations of the adapting gratings substantially habituate magenta transmitters in the LGN (shown as squares that are filled in by smaller black areas in Pathway 2). This habituation of neurons is the basis of the model's explanation of the ME, as in so-called fatigue models. At this point, a natural question is, how can the long duration of the ME, which is clearly longer than the time scale of transmitter depletion and recovery, be explained?

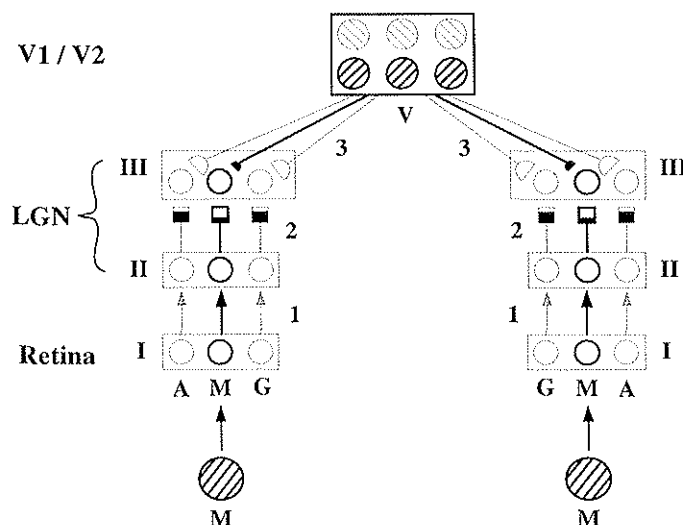


Figure 2: Schematic diagram of corticogeniculate learning in the model in response to  $45^\circ$  binocular gratings of magenta and black stripes. Cells and pathways that are stimulated by the adapting gratings are drawn in bold lines. Unstimulated cells and pathways are drawn in thin lines. Open hemicircles denote the adaptive synapses that have not learned under current adaptations. Filled hemicircles denote the adaptive synapses that have learned under current adaptations. In order to facilitate the explanation, the illustration is simplified in the following ways: (1) only the relevant stages (up to Stage V) of the model are depicted; (2) variable strengths of binocular and monocular cortical cells are not depicted. See text for details.

The model proposes that corticogeniculate feedback pathways (Pathway 3) possess adaptive synapses (shown as hemicircles at the end of Pathway 3) that learn long-term changes in synaptic efficacy. The synaptic strength is hypothesized to track the transmitter-gated signal. Since the transmitter habituates, the net result of these changes is a weakening of the synaptic strength. In this way, a transient magenta transmitter habituation is encoded in the long-term synaptic efficacy in the corticogeniculate feedback pathways that project to magenta LGN cells (shown as smaller filled hemicircles in Pathway 3), while the synaptic efficacy of feedback pathways to green LGN cells remains unchanged (shown as larger open hemicircles in Pathway 3).

On test trials, both the magenta and green retinal cells are equally activated by an achromatic test grating. The synaptic learning caused by prior magenta adaptation, however, causes smaller output signals to be generated from magenta LGN cells than from green LGN cells. Since the output signals from LGN cells are then opponently processed, a net green monocular color signal is generated. When the net green signals from each eye are then binocularly summated and filled in at the binocular FIDO, a green aftereffect is observed. Since the synaptic change, or learning, is driven by transmitter habituation, which is a cumulative process, the learning is also a cumulative process. This property is consistent with the data of Skowbo and White (1983), who showed that the acquisition of the ME depends on the duration, not on the number, of adapting stimulus presentations.

How can the orientation sensitivity of the ME be explained? This property of the ME comes from the orientation sensitivity of BCS cells. Since the gratings used in ME experiments involve only two orientations that are mutually perpendicular, the orientation sensitivity of BCS cells is modeled in a simple way, such that each BCS cell responds to one orientation, but not to the other. For example, when a  $45^\circ$  grating is presented, a subpopulation of BCS cells that are tuned to  $45^\circ$  orientation becomes activated while a subpopulation of cells that are tuned to  $135^\circ$  orientation is inactive, and vice versa. Since the synaptic learning in the corticogeniculate feedback pathway is proposed to take place only when V1 (presynaptic) cells and LGN (postsynaptic) cells are con-

currently active, the synaptic learning becomes contingent on orientation. An adaptation to a 45° magenta grating, for example, leads to the weakening of synaptic strength along the pathways from 45°-specific V1 cells to magenta LGN cells, but not along the other pathways. Therefore, a green aftereffect is observed with a 45° test grating, but not with a 135° test grating. Similarly, an adaptation to a 135° green grating elicits a magenta aftereffect only when tested with a 135° test grating, but not with a 45° test grating.

There are three types of adaptive pathways in the model. One is the corticogeniculate feedback pathway, another is the cortical bottom-up FCS pathway, and the third is the binocular boundary pathway. As described above, the general ME properties – namely, how the effect is typically complementary to the adapting color, and how the effect becomes long-lasting and contingent on orientation – can be explained by using the adaptive mechanisms of the corticogeniculate feedback pathway, or indeed any other early boundary-to-surface pathway with similar properties. What role, then, do the cortical bottom-up FCS pathway and the binocular boundary pathway play for the ME? We propose that the adaptive mechanisms in these pathways play a critical role in explaining anomalous ME data of MacKay and MacKay (1973) and of White *et al.* (1978), but not in explaining the general ME properties described above. In order to see why, it is first necessary to examine the functional role of these pathways in the model.

As proposed by Grossberg (1987), a key function of the adaptive mechanisms in the cortical bottom-up FCS pathway is to establish and to maintain selective contacts between monocular FCS cells and binocular FCS cells that code the same spatial positions and color. Thus achromatic cells map into achromatic cells, magenta cells map into magenta cells, and green cells map into green cells, all at the corresponding spatial positions. Without establishing and maintaining the proper topographic mappings within the featural systems, surface perception would be erroneous both in its spatial position and color.

The reason why the adaptive mechanisms of the cortical bottom-up FCS pathway do not play a critical role in explaining the core issues in the ME comes from the fact that, in typical ME experiments, the adapting gratings presented to the two eyes are of the same color. In such cases, the color registered in the monocular FCS and the color registered in the binocular FCS agree with each other. For example, magenta cells in the monocular FCS are normally connected to magenta cells in the binocular FCS. What happens when magenta adapting gratings are presented binocularly? Such gratings would activate magenta cells in both the monocular FCS and the binocular FCS. Therefore, magenta cells in the monocular FCS continue to connect to magenta cells in the binocular FCS, and the cortical bottom-up FCS pathway is largely unaltered. The same explanation holds also for monocular adaptations, since the monocular color and the binocular color also agrees with each other in such cases.

The role of the cortical bottom-up FCS pathway is best revealed when the colors presented to the two eyes are different, as in the experiments of MacKay and MacKay (1973) and of White *et al.* (1978). The adaptive mechanisms of the binocular boundary pathway also play a critical role in explaining the experiments of MacKay and MacKay (1973). These points will be developed in detail later in this article.

## 2.4 Summary of the McLoughlin Model

Since the simulation results from the McLoughlin model (McLoughlin, 1995) are compared to the FACADE simulations in this article, a brief summary of the McLoughlin model is next described before presenting the FACADE simulations. Figure 3 provides an overview of the McLoughlin model. As can be seen by comparing Figure 2 to Figure 3, there are both similarities and differences between the FACADE and the McLoughlin model. The processing stages in the McLoughlin model are next described before comparing the two models.

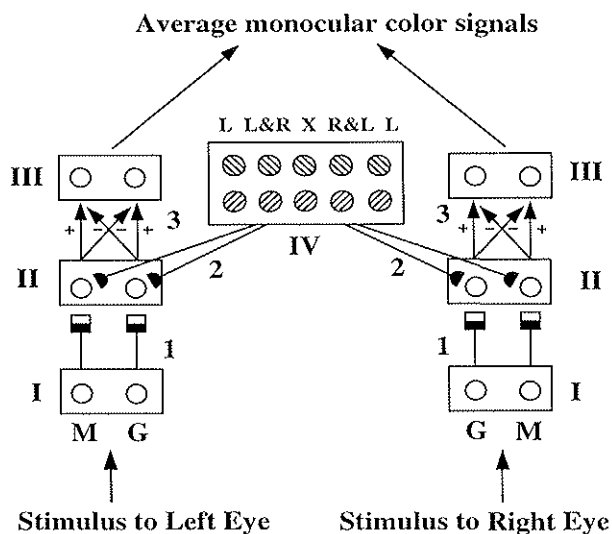


Figure 3: Schematic diagram of the McLoughlin model. Adapted from McLoughlin (1995) with permission. The illustration follows the same conventions used in Figure 1. See text for details.

The model consists of two subsystems: the monocular chromatic subsystem (Figure 3, Stage I, II, and III) and the achromatic subsystem (Figure 3, Stage IV). The first stage (Figure 3, Stage I) is activated by chromatic signals of input stimuli. The achromatic subsystem is activated by orientational signals of input stimuli. Five types of binocularity are simulated: exclusively monocular left (L) and right (R) cells, exclusively binocular (X) cells, and weighted left (L&R) and right (R&L) binocular cells. Upon prolonged presentation of adapting stimuli, transmitters (Figure 3, Pathway 1) substantially habituate, and adaptive weights (Figure 3, Pathway 2) from the achromatic subsystem to the monocular chromatic subsystem become weakened. On test trials, both the magenta and green cells in Stage I are equally activated by an achromatic test grating. However, the synaptic learning caused by prior adaptation causes smaller output signals (Figure 3, Stage II) to be generated from the adapted chromatic channel than from the unadapted chromatic channel because the learned synaptic weights, gated by achromatic system activities, are added to the chromatic channel activities. Opponent processing yields a net monocular color signal which is complementary to the adapting color. The monocular color signals from the two eyes are then arithmetically averaged, which then compared to experimental data.

There are several similarities between the McLoughlin model and the FACADE model: (1) complementary color aftereffects arise due to habituating transmitter gates and opponent processing; (2) the effects are long-lasting because a transient transmitter habituation is encoded in long-term synaptic weights; and (3) the effects become contingent on orientation because synaptic learning takes place only when orientational (presynaptic) and color (postsynaptic) cells are concurrently active. With these similarities, the McLoughlin model explains the general ME properties in much the same way as the FACADE model. Nevertheless, there are important differences between the two models. One is the scope of the model. The McLoughlin model is developed solely for the purpose of explaining the ME. The FACADE model, however, has a much broader aim and explanatory power, which are described earlier in this article. Therefore, the McLoughlin model inevitably adopted simplified schemes in processing visual stimuli: such as, (1) the network is not spatially distributed; (2) there is no specification regarding how the separately processed orientation and color signals are recombined; and, (3) there are no processing stages for binocular color. The third simplification is especially notable because it leads to the model's failure to explain interocular properties of the ME, which will be described later in this article.

Another difference concerns the nature of interaction between the orientational system and the monocular chromatic system. In the FACADE model, feedback from the BCS *multiplicatively* gates the FCS activity. Thus, oriented boundary activity can only modulate the activity of chromatic cells that already receive retinal input. Neurophysiological data supporting such a multiplicative interaction exist (Przybyaszewski *et al.*, 2000; Sillito *et al.*, 1994). In the McLoughlin model, the achromatic subsystem *additively* influences chromatic system activity. Thus, an oriented input to one eye alone can activate monocular chromatic cells of the other eye, even in the absence of retinal input to the latter eye (e.g., when the former eye is tested while occluding the latter eye). This difference between the two models yields different explanations and simulations of some cases, as will be described later.

### 3 Quantitative Model Explanations and Computer simulations of Multiple ME Cases

Thirteen cases of ME experiments from McLoughlin (1995) were simulated in order to examine how closely simulations of the present model match experimental data. Simulations of the model were performed using the equations presented in the Appendix with a single set of numerical parameters. Differential equations of the model were solved either at equilibrium or by numerical integration, as described in the Appendix.

One-dimensional spatial distributions of stimuli for each of the thirteen experiments were used as inputs to the neural network. Opponent-processed filled-in activities of binocular FIDO color cells comprised the final outputs from the network. Such filled-in activities observed in response to achromatic test gratings correspond to the color aftereffects observed in the ME experiment; that is, red filled-in binocular FIDO activities at the positions corresponding to the white stripe regions of achromatic test gratings indicate a red aftereffect, and green activities indicate a green aftereffect. The filled-in value corresponding to the middle spatial position in the white stripe regions was compared to the experimental data, which describe the relative strengths of aftereffects. Since the filled-in regions are flat, other measures (such as an average of filled-in values in the white stripe regions) would yield nearly the same value as the filled-in value at the middle spatial position in the white stripe regions.

For each of the thirteen cases of ME experiments simulated herein, three phases of simulations were necessary; namely, the Weight-Initialization Phase, Adaptation Phase, and Test Phase. During the Weight-Initialization Phase, initial values of all synaptic weights are learned. Weight-initialization strives to learn weight values that the system would have learned under normal conditions; that is, prior to ME adaptations. Weights first start out small and equal for all spatial locations in the network, followed by training of the network until a proper topographic mapping between the BCS and the FCS is established. Gratings are used as the training stimuli with the same amplitude and pattern as the gratings used in ME adaptations. For example, 45° magenta gratings are used to train all the pathways that involve cells for 45° orientations and magenta colors. The same is true for other orientation and color. Weight-initialization learning employs binocular gratings and no transmitter habituation because humans usually view the world binocularly and do not usually stare at objects long enough to cause major amounts of transmitter habituation. In response to the training stimuli, topographic mappings in the three adaptive pathways self-organize according to the correlated activities of their presynaptic and postsynaptic neurons. The values of the self-organized weights are the initial values with which ME adaptation and learning subsequently take place.

During the Adaptation Phase, adapting stimuli are presented to the network for a prolonged length of time. As a result, transmitter becomes habituated and the weights in the three adaptive

pathways change in strength according to the correlated activities of their presynaptic and postsynaptic neurons. Five minutes of adaptation corresponds to twenty iterations of numerical integration. Among the thirteen cases of ME experiments, some employ five minutes of adaptation and others employ longer adaptation. In the simulations, it will be seen how longer adaptation, implemented by a larger number of iterations, leads to more transmitter habituation and learning, resulting in stronger aftereffects.

During the Test Phase, transmitter levels are set to an initial resting level while keeping learned synaptic weights in the three adaptive pathways, on the premise that transmitter dynamics are transient and learned synaptic efficacy is a long-term effect. As a result of prior learning, achromatic test gratings elicit chromatic outputs from the network, whose measure was described earlier. The output measure is then compared to the experimental data. In all thirteen experiments and simulations, the following procedures commonly apply: (1) the strengths of aftereffects are obtained using test gratings shown to the left eye only (left monocular test), to the right eye only (right monocular test), and to both eyes (binocular test); and (2) the strength of aftereffect from the binocular test in the Standard Binocular Case, shown in Figure 3, is used to normalize all other results as a percentage value.

Although there are many parameters in the model, the parameters for the BCS cell activities under monocular and binocular stimulations ( $B_B$ ,  $B_M$ ,  $M_M$ ,  $M_B$ ) have been of particular interest because they play a crucial role in governing the relative strengths of corticogeniculate learning in the several types of feedback pathways during adaptation, and how strongly LGN activities are gated during test. Thus, they were the key parameters that were thoroughly analyzed in the simulations to fit the experimental data. They were chosen in the range between 0 and 1, under the intuitive constraints that  $B_B > B_M$  (binocular cells are more active under binocular stimulations than monocular stimulations),  $M_M > M_B$  (monocular cells are more active under monocular stimulations than binocular stimulations),  $B_B > M_B$  (binocular cells are more active under binocular stimulations than monocular cells), and  $M_M > B_M$  (monocular cells are more active under monocular stimulations than binocular cells). The parameter values were searched beginning with the Standard Binocular Case. Once a set of parameter values was obtained that successfully fit the data from the Standard Binocular Case, a parameter search for the Standard Monocular Case was next done within the previously obtained set, and so on, until the simulation results fit the data from all cases. Each successive parameter search narrowed down the set of parameter values that work for multiple cases. The parameter search was mostly done both empirically and automatically. Empirical understanding of the network dynamics was applied in the parameter search. For example, increasing  $B_B$  was expected to yield an increase in aftereffects in cases where binocular adaptations were employed, and so forth. Automatic parameter search was done so that simulations for all the thirteen cases were automatically repeated for each of the possible parameter combinations, in order to find the set of parameter values that worked best for multiple cases. This being said, it must be realized that the successful parameter sets were not necessarily optimal, since we know no method for optimizing such a complicated data fit using a hierarchically organized network with multiple spatial and temporal scales.

### 3.1 Standard Binocular Case

In the Standard Binocular Case, the two eyes are adapted to the same binocular adapting gratings. A pair of such gratings of opposite color and orientation (that is,  $45^\circ$  magenta gratings and  $135^\circ$  green gratings) is sequentially alternated for five minutes. Thus, each grating is presented for two and one-half minutes. Unless stated otherwise, all experiments simulated in this article use two and one-half minutes as an adaptation time for each grating of a given configuration. Figure 4 summarizes the adapting stimuli (where C1 and C2 refers to the configuration of each adapting

grating), along with a plot showing the experimental data from two subjects (RS and MB) with standard deviations, simulation results from McLoughlin (1995), and simulation results from the present model (FACADE), all under binocular test (Bino), right monocular test (RightMono), and left monocular test (LeftMono).

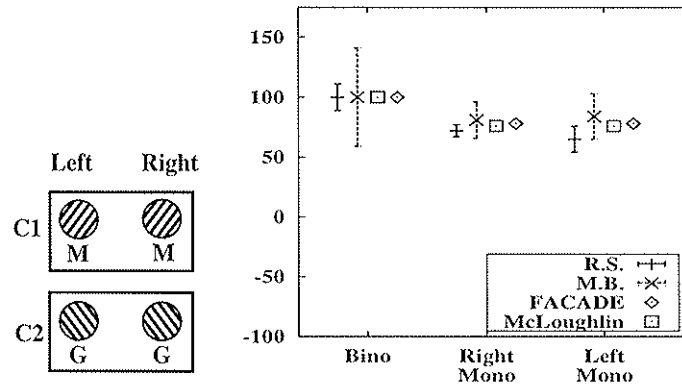


Figure 4: Standard Binocular Case: (Left) Adapting stimuli used. (Right) Experimental data and simulation results for the McLoughlin and FACADE models.

The main finding of the Standard Binocular Case is that the aftereffect induced by binocular adaptations is stronger in the binocular test than in the monocular test. This is explained in the present model as follows. During binocular adaptations, synaptic learning takes place in both of the corticogeniculate feedback pathways that project to the left and the right LGN. Upon binocular test, both learned pathways are used, since LGN cells in both eyes are stimulated by binocular test gratings. Therefore, monocular color signals are generated by both eyes. Upon monocular test, on the other hand, only one of the two pathways is used. Thus, monocular color signals are generated only by one eye. By the process of nonlinear binocular brightness summation (Grossberg & Kelly, 1999), the summated binocular color signals become greater in the binocular test than in the monocular test, although such a summation is not linear. When such binocular color signals are subsequently filled-in, the aftereffect becomes greater in the binocular test than in the monocular test. We have also investigated how the strength of the aftereffect is influenced by presenting the same binocular adapting gratings twice as long. Figure 5 displays the results.

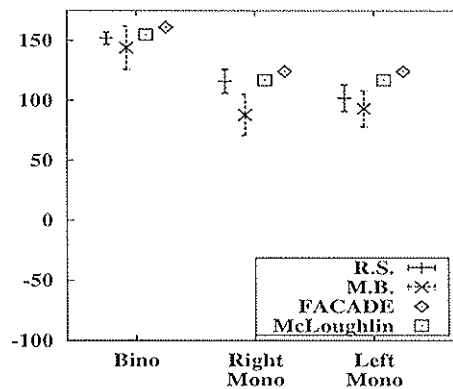


Figure 5: Standard Binocular Case with longer adaptation: Experimental data and simulation results the McLoughlin and FACADE models. The same adapting stimuli as in the Standard Binocular Case is used while adaptation period is made twice as long.

By comparing Figure 5 to Figure 4, it can be seen that the aftereffects become stronger when the adaptation period is made twice as long. This is true in the model because both the transmitter habituations in the LGN and the resultant synaptic changes in the corticogeniculate feedback pathways are cumulative processes that depend on the duration of adapting stimulus presentations.

### 3.2 Standard Monocular Case

The Standard Monocular Case shows that monocular adaptations yield an aftereffect in the adapted eye, but not in the unadapted eye. Here, only the right eye is adapted to monocular gratings. A pair of such gratings of opposite color and orientation is sequentially alternated. Figure 6 summarizes the stimuli and results.

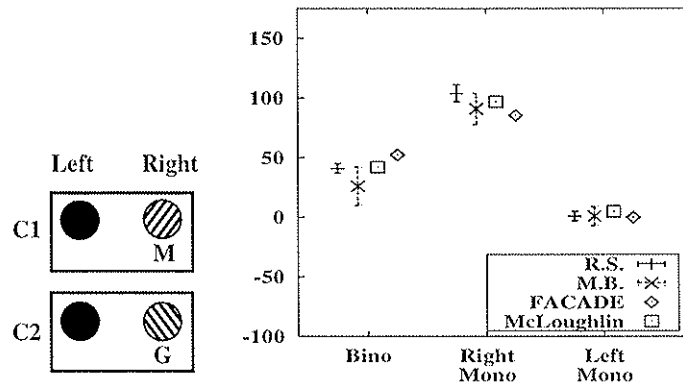


Figure 6: Standard Monocular Case: (Left) Adapting stimuli used. (Right) Experimental data and simulation results for the McLoughlin and FACADE models.

As shown in Figure 6, the aftereffect is confined to the adapted eye only (the right eye). Why does interocular transfer not occur? The model explains the absence of interocular transfer by the architecture of the model and the learning law that is used. Figure 7 shows what happens to the network during monocular adaptations. In particular, synaptic learning occurs in the corticogeniculate feedback pathway only when V1 (presynaptic) cells and LGN (postsynaptic) cells are concurrently active. Since LGN cells in the unadapted left eye are inactive during the right monocular adaptation, no synaptic learning occurs in the corticogeniculate feedback pathway projecting to the left LGN (shown as dashed thin lines that end in open hemicircles in Figure 7). Also, since the left monocular cortical cell is inactive during the right monocular adaptation, no synaptic learning occurs in the corticogeniculate feedback pathway projecting from the left monocular cell (shown as an absence of the left monocular cell and of its feedback pathway). Thus, the aftereffect is not observed in the unadapted left eye, and therefore does not transfer interocularly.

How, then, does the binocular test yield a weaker aftereffect than does the right monocular test? This weaker binocular aftereffect comes from the property that binocular cells are less active than monocular cells under monocular stimulations (shown as smaller "B" compared to larger "R" in Figure 7). Since synaptic learning is gated by activities of both V1 (presynaptic) cells and LGN (postsynaptic) cells, less synaptic learning occurs when V1 cell activity is low. Hence, the adaptive synapses weaken less in the feedback pathway from the binocular cell to the right LGN cell (shown as larger synaptic weight in Figure 7) than in the feedback pathway from the right monocular cell to the right LGN (shown as smaller synaptic weight in Figure 7). Since a binocular test grating strongly stimulates binocular cells and weakly stimulates monocular cells, the binocular test strongly recruits the smaller magnitude of synaptic learning in the binocular feedback pathway

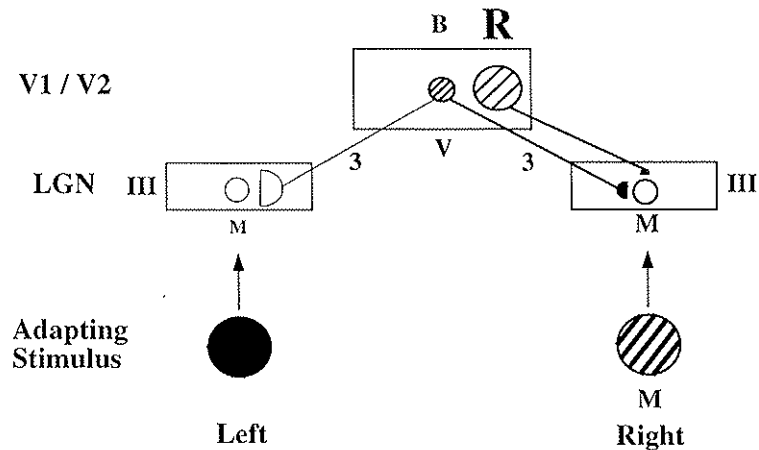


Figure 7: Schematic diagram of corticogeniculate learning in the model in response to right monocular adaptations with a  $45^\circ$  grating of magenta and black stripes. Illustration follows the conventions used in Figure 2. The right monocular adapting grating elicits: (1) transmitter habituation in the right LGN; and (2) a strong activation of the right monocular cell (denoted by large **R**), a weak activation of the binocular cell (denoted by small **B**), and no activation of the left monocular cell (denoted by an absence of **L**). Therefore, the pathway from the right monocular cell to the right LGN shows a larger amount of learning (expressed as a larger weakening in synaptic strength), the pathway from the binocular cell to the right LGN shows a smaller amount of learning (expressed as a smaller weakening in synaptic strength), and the pathways to the left LGN shows no learning (expressed as no change in synaptic strength). See text for details.

and weakly recruits the larger magnitude of synaptic learning in the right monocular feedback pathway. The right monocular test, on the other hand, strongly recruits the larger magnitude of synaptic learning in the right monocular feedback pathway and weakly recruits the smaller magnitude of synaptic learning in the binocular feedback pathway. Therefore, the binocular test yields a weaker aftereffect than the right monocular test does, after right monocular adaptation.

It should be noted that the McLoughlin simulation elicits a small (5%) aftereffect upon testing the unadapted left eye whereas the FACADE simulation does not. This difference arises because each model uses different mechanisms whereby learned weights in the orientational system influence chromatic activities: learned weights additively activate chromatic activities in the McLoughlin model, whereas they multiplicatively modulate in the FACADE model. Therefore, in the McLoughlin model, chromatic activities can arise in an eye's projections even when that eye is occluded, providing that the other eye is presented with an orientational stimulus which activates the binocular achromatic subsystem.

How do these different mechanisms contribute to the different simulation results? In both models, learning occurs along the pathways from the binocular orientational system to the monocular chromatic system of the adapted right eye. Upon testing the unadapted left eye by presenting the test grating to the left eye while occluding the adapted right eye, no effect is elicited from the unadapted left eye in both models because the pathways to the left chromatic system were not learned. From the right eye which was adapted but is occluded during test, however, an effect is elicited in the McLoughlin model but not in the FACADE model. Due to the orientational stimulus to the left eye, the orientational system, which is binocular in both models, becomes activated. Once activated, it sends signals along the learned pathways to the monocular chromatic system of the occluded right eye, which receives no retinal input. In the McLoughlin model, an effect is elicited from the right eye due to the additive nature of the modulatory signals, although the effect is small because not all weights learned during right adaptation are activated during left test;

e.g., the strongest learning occurred at R (exclusively monocular right) weights, but they are not recruited during left test. In the FACADE model, no effect is elicited from the right eye due to the multiplicative nature of the modulatory signals. Therefore, there is no interocular transfer of the ME under monocular adaptation in the FACADE model, as reported in the data of McCollough (1965).

### 3.3 Monocular Same Case

In the Monocular Same Case, the two eyes are adapted to the same monocular adapting gratings. A pair of such gratings of opposite color and orientation is sequentially alternated. Figure 8 summarizes the stimuli and results. Comparing the results from the Monocular Same Case with the Standard Monocular Case, it can be seen that the monocular test scores are about the same in both cases, but the binocular test score is greater in the Monocular Same Case than in the Standard Monocular Case. This difference arises in the model because, the feedback pathways projecting to both the left and the right LGN are learned in the Monocular Same Case, whereas only the feedback pathways projecting to the right LGN are learned in the Standard Monocular Case. Therefore, after opponent processing, a binocular test in the Monocular Same Case elicits adapted monocular color signals from both eyes, whereas a binocular test in the Standard Monocular Case elicits monocular color signals from the right eye only. After binocular summation, binocular color signals become greater in the Monocular Same Case than in the Standard Monocular Case. Accordingly, the binocular test score becomes greater in the Monocular Same Case than in the Standard Monocular Case.

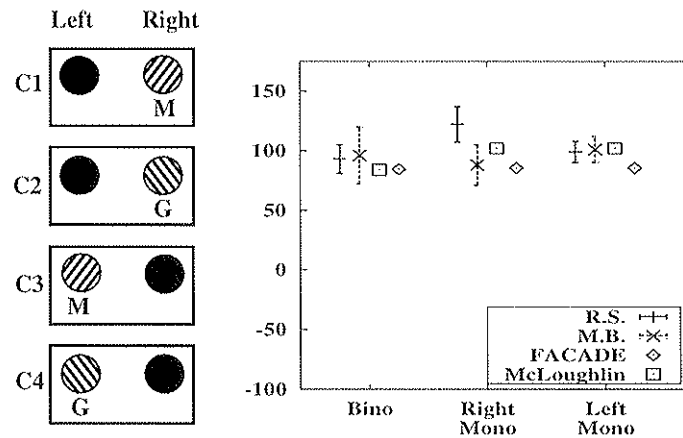


Figure 8: Monocular Same Case: (Left) Adapting stimuli used. (Right) Experimental data and simulation results for the McLoughlin and FACADE models.

### 3.4 Monocular Opposite Case

In the Monocular Opposite Case, the two eyes are adapted to opposite monocular adapting gratings. A pair of such gratings of opposite color and orientation is sequentially alternated. Figure 9 summarizes the stimuli and results. As shown in Figure 9, the binocular test score is around zero and the two monocular tests yield opposite effects. The left monocular test score is plotted on the negative axis to emphasize that the aftereffect color in the left test is opposite to the color in the right test. The present theory explains the opposite monocular test results just as in the Monocular Same Case; namely, using the learning mechanism in the feedback pathways. The monocular aftereffects in the Monocular Opposite Case exhibit opposite colors because the feedback pathways

projecting to the two eyes learn from the transmitter habituation of opposite colors. For example, for the C1 stimulus in Figure 9, the  $45^\circ$ -specific feedback pathways to the right LGN learn from habituated magenta activities, whereas for the C3 stimulus in Figure 9, the  $45^\circ$ -specific feedback pathways to the left LGN learn from habituated green activities. Therefore, testing the right eye with a  $45^\circ$  achromatic grating elicits a green aftereffect, whereas the left monocular test elicits a magenta aftereffect. The same explanation holds for the zero binocular test score. Upon a binocular test with a  $45^\circ$  achromatic grating, green and magenta monocular signals are generated from the right and left eye, respectively. These oppositely colored monocular signals cancel out when they are binocularly summated and opponently processed (Figure 1, Pathway 7).

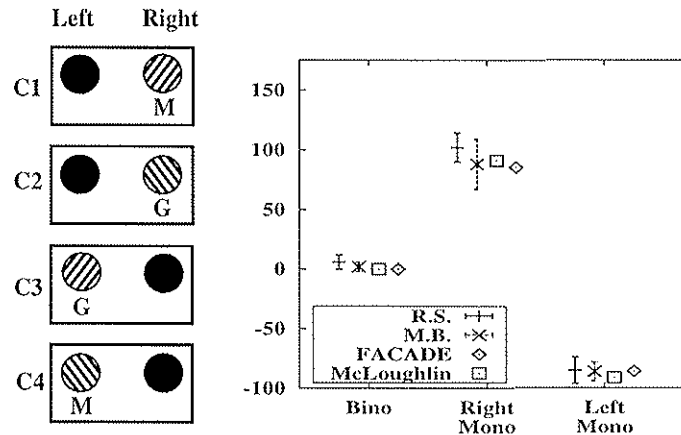


Figure 9: Monocular Opposite Case: (Left) Adapting stimuli used. (Right) Experimental data and simulation results for the McLoughlin and FACADE models.

### 3.5 Binocular and Monocular Opposite Case

This case replicates an experiment of Vidyasagar (1976), who was the first to demonstrate that a binocular locus is involved in the ME by showing that the binocular aftereffect can be made opposite to the monocular aftereffect. In this experiment, the two eyes are adapted not only to monocular adapting gratings, but also to binocular adapting gratings whose configurations are opposite to the monocular adapting gratings both in orientation and color. A pair of these gratings of opposite color and orientation is presented. Figure 10 summarizes the stimuli and results.

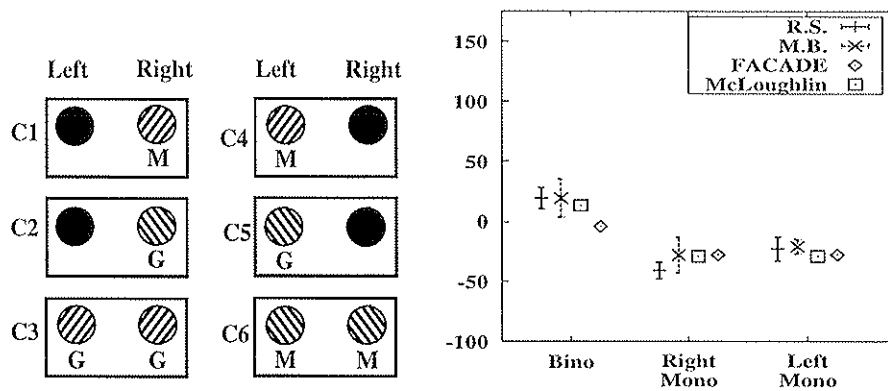


Figure 10: Binocular and Monocular Opposite Case: (Left) Adapting stimuli used. (Right) Experimental data and simulation results for the McLoughlin and FACADE models.

As shown in Figure 10, the binocular test and the two monocular tests yield small aftereffects even though the adaptation period is made much longer, employing six adapting stimuli. The effects are small in the model because, for each orientation, BCS cells learn the transmitter habituation of both colors whose learned effects subsequently compete with each other via opponent processing, leading to smaller net aftereffects. For example, for stimuli C1 and C4 in Figure 10, BCS cells tuned to  $45^\circ$  learn from habituated magenta activities, whereas for the C3 stimulus, the same BCS cells learn from habituated green activities. Opponent processing of the two opposite learned effects results in smaller net aftereffects.

The binocular and monocular effects also tend to be opposite because the binocular cells learn more strongly from the color of the binocular adapting gratings, and the monocular cells learn more strongly from the color of the monocular adapting gratings. For example,  $45^\circ$ -specific binocular cells learn strongly from habituated green activities (the binocular C3 stimulus) and weakly from habituated magenta activities (the monocular C1 and C4 stimuli). Therefore, a binocular test with  $45^\circ$  test grating tends to yield a small magenta aftereffect because binocular test strongly recruits binocular cells. Likewise, a monocular test with  $45^\circ$  test grating tends to yield a small green aftereffect.

It should be noted, however, that the tendency for binocular and monocular tests to yield opposite aftereffects depends on the parametric values of binocular and monocular BCS cells. It is true that, regardless of parametric values, binocular cells learn more strongly from the color of binocular adaptation gratings than from the color of monocular adaptation gratings, and monocular cells learn more strongly from the color of monocular adaptation gratings than from the color of binocular adaptation gratings. In other words, as far as adaptation and learning are concerned, binocular and monocular cells themselves learn more preferentially from the two opposite colors, regardless of their parametric values. This is because of the constraints that  $B_B > B_M$  (binocular cells are more active under binocular stimulations than monocular stimulations),  $M_M > M_B$  (monocular cells are more active under monocular stimulations than binocular stimulations).

Aftereffects elicited by binocular and monocular tests, however, do depend on the parametric values of binocular and monocular BCS cells under binocular and monocular stimulation conditions. If BCS cells were exclusive (e.g., binocular stimulations activate binocular cells, but not monocular cells, vice versa), binocular test would yield an aftereffect complementary to binocular adapting color and monocular test would yield an aftereffect complementary to monocular adapting color, regardless of parametric values. Since BCS cells are not exclusive, however, it is needed to take into account of the activities of the two types of BCS cells under the two types of stimulation conditions. Therefore, aftereffects are parameter-dependent. For example, strong  $M_M$  (monocular cell activity under monocular stimulations) and  $B_M$  (binocular cell activity under monocular stimulations) causes strong learning during monocular adaptation and strong recruitment of BCS cells during monocular test. In such case, monocular adaptational effects outweigh binocular adaptational effects, leading to a very small binocular test score which may not be opposite to monocular test scores, as shown in Figure 10. This small deviation of simulations from experimental data is purely a parametric problem which occurs when fitting data from multiple cases with one set of parameters. It just indicates that, under the current set of parameters, monocular adaptational effects outweigh binocular adaptational effects for this particular case. Evidence for the hypothesized role of binocular adaptation can be easily observed in the next case.

In this case, investigations are done on how the strengths of the binocular and monocular aftereffects are influenced by longer binocular adaptations while leaving the monocular adaptations the same, by presenting the same binocular adapting gratings twice as long. Figure 11 summarizes the stimuli and results. By comparing Figure 11 to Figure 10, it can be seen that longer binocular adaptations result in changes in both binocular and monocular tests. In both tests, changes are observed in an upward direction, which means that binocular adaptational effects begin to

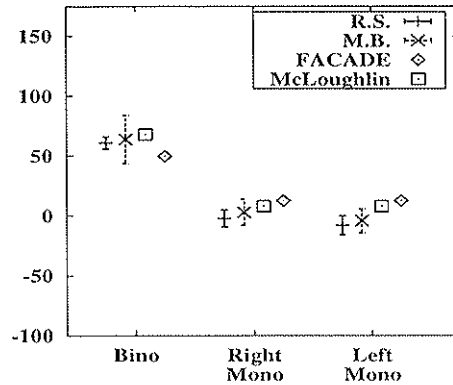


Figure 11: Binocular and Monocular Opposite Case with longer adaptation: (Left) Adapting stimuli used. (Right) Experimental data and simulation results for the McLoughlin and FACADE models. The same adapting stimuli as in the Binocular and Monocular Opposite Case whereas binocular adaptation period is made twice as long.

outweigh monocular adaptational effects. The observation that the binocular aftereffect becomes stronger under longer binocular adaptations is consistent with our explanation of the Standard Binocular Case, where longer adaptations cause longer activation and learning of BCS cells. The observation that the monocular aftereffect reverses its sign from Figure 10 to Figure 11 indicates that the effects of longer binocular adaptations eventually predominate over the effects of relatively shorter monocular adaptations. This observation that monocular aftereffects are influenced by longer binocular adaptations to the opposite color and orientation provides strong evidence for opponent color processing, and for the activation of binocular cells by monocular inputs. In other words, the binocular cells should be “OR” in their nature. This case also provides evidence that the small deviation of simulations from experimental data observed in the previous case is purely a parametric problem. In the previous case, the deviation indicates that, under the current set of parameters, monocular adaptational effects outweigh binocular adaptational effects. With longer binocular adaptations in the present case, binocular adaptational effects now outweigh monocular adaptational effects, fitting the experimental data well.

The McLoughlin model explains the Binocular and Monocular Opposite Case in much the same way as the FACADE model because of the similarities between the two models, as were described earlier. The better fits obtained by the McLoughlin model are purely parametric effects due to its simpler simulation environment. The learned connections subserving this case are similar to those in the FACADE model, as is the BCS-to-(monocular FCS) learning in the FACADE model to the (achromatic subsystem)-to-(monocular chromatic subsystem) in the McLoughlin model.

### 3.6 Anomalous ME Case

The Anomalous ME Case replicates an experiment of MacKay and MacKay (1973), who showed that the ME can be generated by presenting color and orientational information separately to the two eyes. The left eye is adapted to a sequentially alternating pair of homogeneous colored fields. The right eye is adapted to a sequentially alternating pair of achromatic gratings. Figure 12 summarizes the stimuli and results. The absence of a McLoughlin simulation in Figure 12 indicates that the McLoughlin model cannot explain the anomalous ME because the color system in the McLoughlin model is strictly monocular. The extra degrees of freedom that are needed to binocularly align and fuse monocular color signals to form a final binocular percept make it harder to simulate all the cases with a single set of parameters.

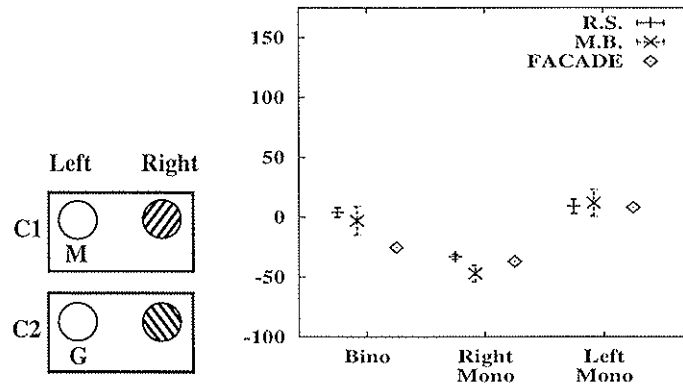


Figure 12: Anomalous ME Case: (Left) Adapting stimuli used. (Right) Experimental data and simulation results for the FACADE model.

As shown in Figure 12, chromatic aftereffects are induced even though neither of the two eyes was given an adapting stimulus containing both orientation and color information. Moreover, the right monocular test yields an anomalous aftereffect (plotted on the negative axis) – that is, its aftereffect was the same hue as the adapting colored field – whereas the left monocular test yields a standard ME. The standard ME observed in the left eye where only color information has been provided during adaptation indicates that orientation information can transfer interocularly. The model explanation of how this happens is illustrated in Figure 13.

The model explains the standard effect in the left test by the activation of binocular cells with monocular inputs, as illustrated in Figure 13. The achromatic grating presented to the right eye activates not only the right monocular BCS cell (labeled as “R” in Figure 13), but also the binocular BCS cell (labeled as “B” in Figure 13). The feedback pathways projecting from the activated binocular BCS cell to the left magenta LGN then learn from the transmitter habituation in the left eye (shown as a weakened synaptic weight in that pathway in Figure 13). Therefore, orientation information can transfer interocularly. Thus, this case provides additional evidence that the binocular cells are “OR” in their nature. Although the aftereffect is observed in the left eye, it is nevertheless weak in the model because of two reasons. First is the “dilution” of the aftereffect by recruiting the left monocular BCS cell whose feedback pathway did not learn during adaptation. The second reason comes from the proposal that binocular cells are less active during monocular stimulations than during binocular stimulations (shown as smaller “B” compared to larger “R”). Therefore, the magnitude of learning in the feedback pathway from the binocular cell to the left LGN is small, which then leads to the smaller aftereffect in the left monocular test.

Having explained how the left monocular test yields a standard aftereffect, it remains to explain how the right monocular test yields an anomalous aftereffect. In this case, the model suggests that learning in the cortical bottom-up FCS pathways to the Binocular Filling-In Domain (FIDO) plays a crucial role, as briefly mentioned earlier in this article. For example, in response to the C1 adapting stimulus, achromatic cells in the right monocular FCS (shown as cell “A” in Stage IV in Figure 13), which are normally connected to achromatic cells in the binocular FIDO, become associated also with magenta cells in the binocular FIDO (shown as a learned synaptic weight in the pathway from cell “A” in Stage IV to cell “M” in Stage VI in Figure 13) which are activated by magenta stimulations in the left eye. Therefore, when the right eye is tested with an achromatic test grating, the magenta cell in the binocular FIDO becomes activated due to the prior association between the right monocular achromatic cell and the binocular magenta cell. The activation of binocular magenta cells leads to a magenta percept after filling-in occurs. The learning in the cortical bottom-up FCS pathways uses the same learning mechanisms that are used for the

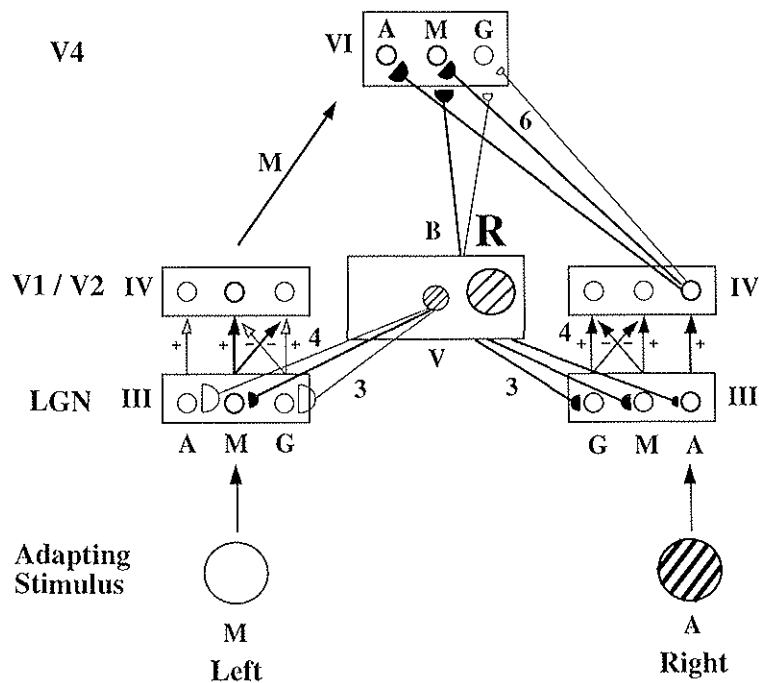


Figure 13: Schematic diagram of corticogeniculate, cortical bottom-up FCS, and binocular boundary learning in the model in response to C1 adapting stimulus of the Anomalous ME Case. Illustration follows the conventions used in Figure 2 and 7. In response to the achromatic grating to the right, binocular cell is activated weakly and right monocular cell is activated strongly. Corticogeniculate feedback pathway from the binocular cell to the left magenta LGN learn from magenta habituation. The homogeneous magenta stimulus to the left also provides magenta signals to the binocular FIDO (illustrated as an "M" arrow from Stage IV in the left to Stage VI). The achromatic grating to the right activates the right achromatic cell in Stage IV. Cortical bottom-up FCS pathway from the activated right achromatic cell to the binocular magenta cell is learned (illustrated as a strengthening of synaptic strength). Binocular boundary pathway from the activated BCS cells to the binocular magenta cells is also learned (illustrated as a strengthening of synaptic strength). Both the learning in the cortical bottom-up FCS pathway and the binocular boundary pathway are involved in the anomalous ME.

corticogeniculate feedback pathway; namely, synaptic learning takes place only when both presynaptic and postsynaptic cells are concurrently active, and synaptic strength tracks postsynaptic activity. In this case, the presynaptic cells are monocular FCS cells and the postsynaptic cells are binocular FIDO cells.

Having proposed how learning in the cortical bottom-up FCS pathway contributes to the anomalous aftereffect, it remains to explain how the anomalous aftereffect becomes orientation-contingent. A problem is that the cortical bottom-up FCS pathway, which is a part of FCS system, is not orientation-specific. Hence, it cannot explain the orientation-contingency of the anomalous ME by itself. For example, consider how the cortical bottom-up FCS pathway is learned when both the C1 and C2 adapting stimuli in Figure 12 are sequentially alternated during the adaptation period. Figure 13 illustrates learning in the model only in response to the C1 adapting stimulus only. When stimuli C1 and C2 alternate, the right monocular achromatic cell becomes associated with both binocular magenta and green cells. This association is not orientation-specific because the cortical bottom-up FCS pathway is not specific to orientation. When the right eye is then tested with an achromatic test grating of any orientation, both the magenta and green cells in the binocular FIDO become activated, which would yield a net zero aftereffect due to opponent

processing of two opposite filled-in color signals. To explain the anomalous ME, however, one needs to understand how an aftereffect of one color or the other can be elicited, depending on the orientation. What learning mechanism keeps track of which adapting color is presented with which orientation?

The model proposes that the boundary pathways to the binocular FIDO have this property; namely, the pathways from Stage V to Stage VI in Figure 13. The model proposes that these boundary pathways *and* the feature pathways to the Binocular FIDO can undergo learning. The feature learning enables corresponding positions from the left and right eyes to get adaptively aligned for purposes of binocular matching. The boundary learning enables the allelotropically-shifted boundaries to adaptively align themselves with the (relatively) unshifted feature signals. For example, for the C1 adapting stimulus, 45°-specific binocular boundary pathways to the magenta cells in the binocular FIDO become stronger (shown as learned synaptic weights in the binocular boundary pathways to cell "M" of Stage VI in Figure 13). Likewise, 135°-specific binocular boundary pathways to the green cells in the binocular FIDO become stronger during adaptation with the C2 adapting stimulus. In this way, binocular boundaries become stronger only within pathways of correlated orientation and color.

This correlated binocular boundary learning leads to preferential gating of a color signal which has been correlated with a given orientation, over the other color signal which has not been correlated. For example, magenta and green FCS signals of equal strength are elicited in the binocular FIDO upon a right test, due to prior learning within the cortical bottom-up FCS pathway during C1 and C2. Due to orientation-selective boundary gating, when a 45° test grating is used, magenta FCS signals are more strongly gated than green FCS signals, leading to stronger magenta filled-in activities than green filled-in activities. Net magenta activities are obtained upon opponent processing, which correspond to the anomalous ME. The opposite is true for a right test a 135° grating. In short, the cortical bottom-up pathway learns the correlation of a right achromatic FCS signal and binocular FIDO magenta and green signals, and the binocular boundary pathway learns the correlation of an orientation and a binocular FIDO chromatic signal. The learning in the binocular boundary pathway uses the same learning mechanisms that are used for the corticogeniculate feedback pathway and the cortical bottom-up FCS pathway; namely, synaptic learning takes place only when both presynaptic and postsynaptic cells are concurrently active and synaptic strength tracks postsynaptic activity. In this case, the presynaptic cells are BCS cells and the postsynaptic cells are binocular FIDO cells.

Even though the same learning law is used in both the corticogeniculate feedback pathway and the binocular bottom-up pathway, the former become weakened whereas the latter become strengthened during adaptation. How do these opposite learning effects happen? The model proposes that this is due to the nature of the ongoing learning and decay which adaptive pathways in the model are conceptualized to undergo. In the simulations, synaptic weights of these pathways are set up during the Weight-Initialization Phase, as described earlier. Under normal viewing conditions, correlations between monocular achromatic FCS signals in one eye and monocular chromatic FCS signals in the other eye are very small at the Binocular FIDO. The anomalous ME stimuli force these correlations to grow, and the correlations from boundary cells to the Binocular FIDO grow correspondingly. In contrast, the corticogeniculate boundary-to-(monocular FCS) signals, start out large, and weaken due to prolonged stimulus inspection. In order to implement these differential correlations in a simple way, training stimuli were presented continuously to the network during the Weight-Initialization Phase, and the corticogeniculate feedback pathway was learned until equilibrium was reached. In contrast, learning in the binocular boundary pathway to the FCS was stopped in the middle of learning (at the 50<sup>th</sup> iteration of numerical integration).

### 3.7 Monocular Adaptation with White Field Occlusion

The Standard Monocular Case showed that aftereffects do not transfer interocularly when the unadapted eye is occluded with a black field. Lehmkuhle and Fox (1976) reported that the magnitude of interocular transfer of a motion aftereffect was influenced by the method that was used to block stimulation of unadapted eye. In particular, less interocular transfer was produced by occluding the unadapted eye with a dark field than with a homogeneous luminous field. For this reason, they speculated that occluding the unadapted eye with an achromatic luminous field might reveal interocular transfer in those kinds of aftereffects where transfer had not been previously reported. This possibility was investigated by McLoughlin (1995), who used an achromatic luminous field, rather than a black field, to occlude the unadapted eye. The left eye was adapted to a white luminous field and the right eye to a pair of sequentially alternating monocular gratings of opposite color and orientation. Figure 14 summarizes the stimuli and results.

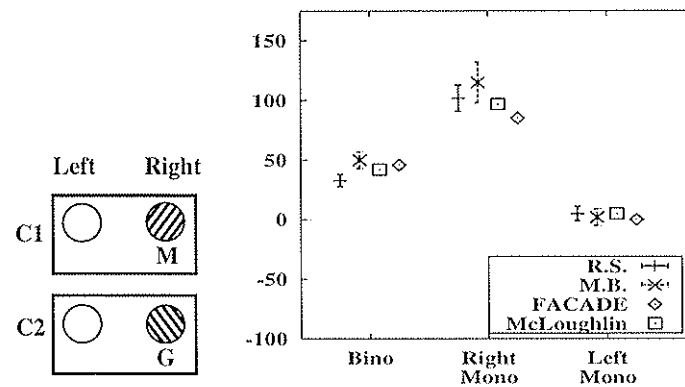


Figure 14: Monocular Adaptation with White Field Occlusion Case: (Left) Adapting stimuli used. (Right) Experimental data and simulation results for the McLoughlin and FACADE models.

As shown in Figure 14, testing the unadapted left eye yielded a nearly zero aftereffect, just as in the Standard Monocular Case. The absence of interocular transfer arises in the model because the white field results in equal habituation within the magenta and green LGN cells. Therefore, the corticogeniculate feedback pathway learning of these equal but opposite habituations is also equal in magnitude. After opponent processing, these equal and opposite effects cancel out. Since interocular transfer is not observed both from the Standard Monocular Case and the present case, it can be said that the interocular transfer of the ME is not influenced by the occlusion method, contrary to the Lehmkuhle and Fox (1976) speculations.

Why is there no aftereffect in the present case, but there are aftereffects in the Anomalous ME Case? Without further model assumptions, there is, in fact, a tendency to yield an anomalous effect when the left eye was tested; that is, the left test can show an aftereffect of the same hue as the adapting colored grating. Figure 15 schematically illustrates what would be learned during adaptations of the present case, unless further assumptions are made. After explaining the problem, we will propose what mechanisms may be at work.

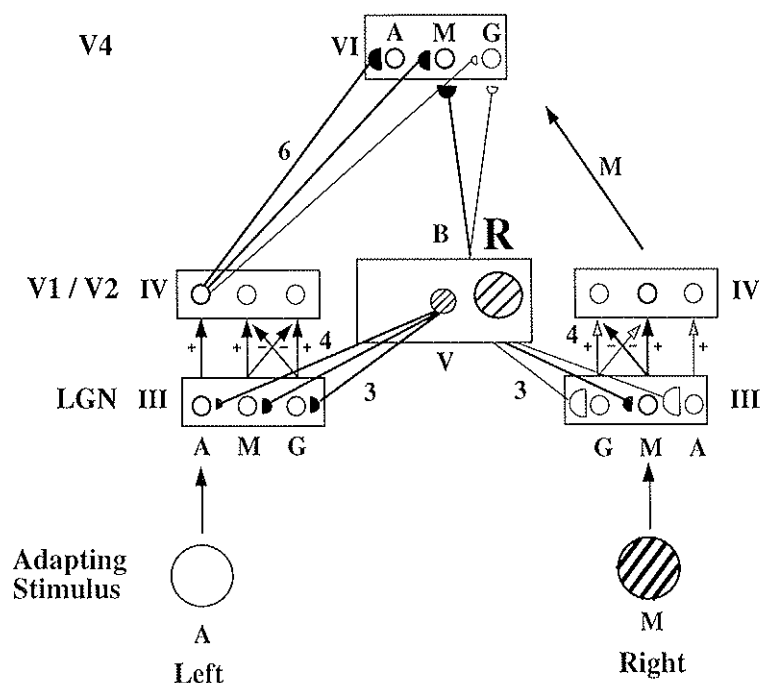


Figure 15: Schematic diagram illustrating why there was a tendency in the simulations to yield an anomalous effect upon left test when it should have yielded no aftereffect in order to fit the experimental data. The figure shows learning in the model in response to the C1 adapting stimulus of Monocular Adaptation with White Field Occlusion Case. Illustration follows the same conventions used in Figure 13. Note that the similarity of network activations and learning between the present figure and Figure 13. See text for details.

As can be seen by comparing Figure 15 with Figure 13, in both the present case and in the Anomalous ME Case, one eye is presented with achromatic color and the other eye with chromatic color. Achromatic monocular FCS cells can hereby become associated with the color presented to the opposite eye at the Binocular FIDO; in particular, an association can occur between the left achromatic FCS cell and the binocular chromatic FCS cell in the present case (Figure 15, Pathway 6). This association is analogous to the association between the right achromatic FCS cell and the binocular chromatic FCS cell in the Anomalous ME Case (Figure 13, Pathway 6). Subsequently, the binocular boundary pathway can learn the correlation of an orientation and a binocular FIDO chromatic signal and thereby become strengthened. The learning in both the cortical bottom-up FCS pathway and the binocular boundary pathway could hereby elicit an anomalous aftereffect, as previously described in detail.

Contrary to this tendency, experimental data presented in Figure 14 shows that no aftereffect is observed in the left test of the present case. What other mechanisms may be at work? How can these mechanisms act without disturbing the model's successful explanations of all other cases? Two assumptions that incorporate properties of the connections which may be expected to develop due to real-world properties of images enable the model to successfully explain the present case while preserving the fit for all other cases.

The first assumption is that learning in the cortical bottom-up FCS pathway occurs more weakly in the pathway from monocular achromatic cells to binocular chromatic cells than in the pathway from monocular achromatic cells to binocular achromatic cells. This assumption is intuitive because a key function of the adaptive mechanisms in the cortical bottom-up FCS pathway is to establish and to maintain selective contacts between monocular FCS cells and binocular FCS

cells that code the same spatial positions and color during normal viewing conditions. Since the two eyes are normally presented with the same color during normal viewing conditions, anatomical connections between monocular and binocular FCS cells that code the same color should be strongly developed. Connections between cells that code different color, however, should be weak and sparse. Therefore, when the two eyes are presented with different colors as in the present case (white to the left eye, color to the right eye), the cortical bottom-up FCS pathway learns weakly, and a spurious anomalous aftereffect will not be elicited in the left test.

If only this assumption is made, however, then not only is the anomalous aftereffect absent in the present case, as desired, but it is also absent in the Anomalous ME Case. One additional assumption helps to explain all the data. It constitutes a prediction for which some compatible data are known, but does not seem to have been directly tested. This assumption is that achromatic channels adapt less than chromatic channels. In order to see why this assumption helps, consider learning in the cortical bottom-up FCS pathway in the Anomalous ME Case and in the present case. As previously stated, synaptic learning in the cortical bottom-up FCS pathway is gated by presynaptic and postsynaptic activities. In the cortical bottom-up FCS pathway, the presynaptic cells are monocular FCS cells and the postsynaptic cells are Binocular FIDO cells. Stronger monocular FCS cell activities lead to faster cortical bottom-up FCS learning. When the achromatic channel is made to adapt weakly, by having less habituation in the transmitter level, corticogeniculate feedback pathways weaken less. The corticogeniculate feedback pathway projecting to the right achromatic FCS cell therefore weakens less during adaptation of the Achromatic ME Case (Figure 13, Pathway 3). As a result, the right achromatic signals yield larger outputs (Figure 13, Cell A of Stage IV). The stronger monocular FCS cell activity causes faster learning in the cortical bottom-up FCS pathway. Thus, the cortical bottom-up pathway from the right achromatic to the binocular chromatic cell (Figure 13, Pathway 6) shows considerable learning despite its weaker anatomical connections, thus eliciting an anomalous aftereffect in the Anomalous ME Case.

There are many possible ways in which achromatic and chromatic channels can differ, including their temporal dynamics, the inputs that they encode, etc. For simplicity, in the simulations, achromatic and chromatic LGN cells were given the same rate parameters, and the differential adaptational property was implemented by smaller transmitter depletion rate ( $\mu_1$  of Equation (11) in the Appendix) in the achromatic LGN cells than in the chromatic LGN cells. There is evidence that rods show less change than cones during adaptation by steady light (Cohn & Lasley, 1986), but little data about whether more central mechanisms also show this predicted difference.

### 3.8 Like Color Case

This case replicates the "like color" experiment of White *et al.* (1978). The left eye is adapted to a sequentially alternating pair of homogeneous colored fields. The right eye is adapted to a sequentially alternating pair of colored gratings of like colors. Figure 16 summarizes the stimuli and results. A main finding of this case is that, even though the left adapting stimuli are devoid of orientational information, the aftereffect is nevertheless observed in the left eye, although the strength of the aftereffect is small. It indicates that orientational information can transfer interocularly using the same mechanisms that were used to explain the Anomalous ME Case; namely, systems that code orientational information (BCS in the the FACADE model, and the achromatic subsystem in the McLoughlin model) are binocular in their nature, which can be activated not only by binocular stimulations but also by monocular stimulations. Therefore, the FACADE model, as well as the McLoughlin model, can explain the interocular transfer of orientational information in this case. Nevertheless, the McLoughlin model cannot explain the Anomalous ME Case because the color system in the McLoughlin model is strictly monocular.

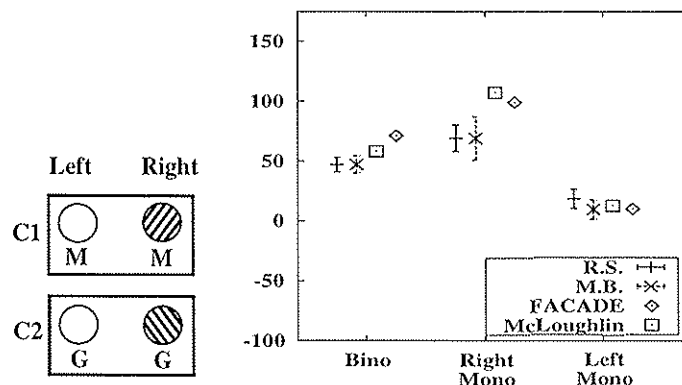


Figure 16: Like Color Case: (Left) Adapting stimuli used. (Right) Experimental data and simulation results for the McLoughlin and FACADE models.

### 3.9 Different Color Case

This case replicates the “different color” experiment of White *et al.* (1978) and is identical to the Like Color Case except that the two eyes see different colors in this case. Figure 17 summarizes the stimuli and results. As shown in Figure 17, a main finding of this case is that the left monocular test yields a zero aftereffect. This effect is explained in the model by combining the adaptive mechanisms of the corticogeniculate feedback pathway and of the cortical bottom-up FCS pathway. As has been explained previously in the Anomalous ME Case and the Like Color Case, the orientational information of adapting stimuli transfers interocularly by virtue of binocular boundary cells which can trigger corticogeniculate feedback learning. For example, in response to the C1 stimulus in Figure 17, learning in the feedback pathway from binocular boundary cells to left green LGN cells would lead to a small magenta aftereffect in the left eye. However, such an effect is not observed in the present case because the learning in the cortical bottom-up FCS pathway cancels it out.

This cancellation happens in the FACADE model as follows. As has been explained in the Anomalous ME Case, magenta and green cells in the monocular FCS are normally connected to magenta or green cells, respectively, in the Binocular FIDO. The dichoptic adaptation to two different colors in the present case, however, re-tunes these connections such that magenta and green cells in the monocular FCS become, to a certain degree, cross-associated to green or magenta cells in the Binocular FIDO, respectively. This cancels out the small magenta effect produced by the feedback learning in response to the C1 stimulus at the left LGN, resulting in a nearly zero aftereffect in the left monocular test, as shown in Figure 17. To summarize, the learning in the corticogeniculate feedback learning and in the cortical bottom-up FCS pathway compete with each other in the present case.

In the McLoughlin model, the same cancellation effect is elicited, but using a different mechanism. It is elicited not by a mechanism involving monocular-binocular color interaction, but as an effect of the previously described additive nature of learned weights in the orientational system, as follows. During the dichoptic adaptation to two different colors, the binocular orientational system learns the habituation of the two different colors presented to each eye. The left test presents the test grating to the left eye while occluding the right eye. Then an effect is elicited from the left eye, and an opposite effect is elicited from the occluded right eye because the learned weights additively activate right chromatic cells which receive no retinal input. By averaging the two opposite monocular effects, a nearly zero aftereffect is elicited in the left monocular test.

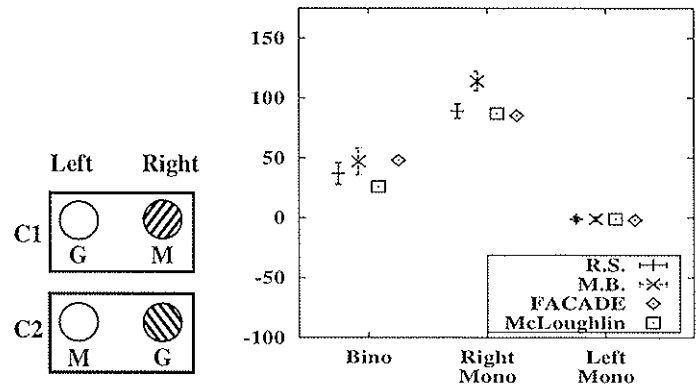


Figure 17: Different Color Case: (Left) Adapting stimuli used. (Right) Experimental data and simulation results for the McLoughlin and FACADE models.

### 3.10 Isoluminant Adaptation Case

This case replicates an experiment of Stromeyer and Dawson (1978) and is identical to the Standard Binocular Case except that the gratings are made of isoluminant colored and gray stripes. Figure 18 summarizes the stimuli and results. As Stromeyer and Dawson (1978) have shown, the use of isoluminant adapting gratings fail to induce the ME. This arises in the model because BCS cells that are sensitive to luminance contrast respond very weakly to isoluminant stimuli. Since BCS cells are not active, learning does not occur in the corticogeniculate feedback pathway; hence, aftereffects are not induced.

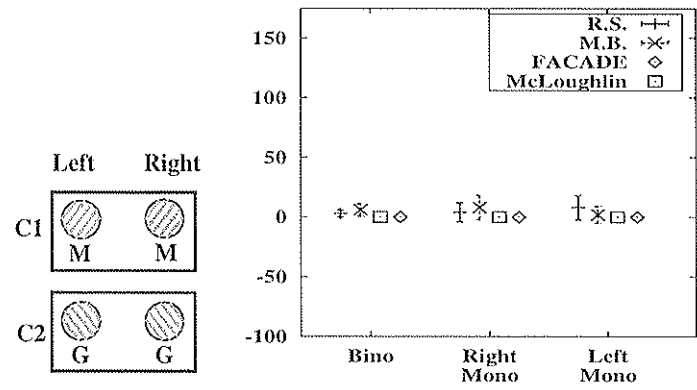


Figure 18: Isoluminant Adaptation Case: (Left) Adapting stimuli used. (Right) Experimental data and simulation results for the McLoughlin and FACADE models.

### 3.11 Binocular Rivalry Case

This case replicates the “different color/different orientation” experiment of White *et al.* (1978). In this case, the two eyes are adapted to opposite binocular adapting gratings. A pair of such gratings of opposite color and orientation is sequentially alternated. Figure 19 summarizes the stimuli and results. As shown in Figure 19, standard aftereffects are observed in both the binocular and the monocular tests although the two eyes see different orientation/color combinations during adaptation. This is explained in the model using the learning mechanisms in the corticogeniculate feedback pathway; namely, the corticogeniculate feedback pathway learns the correlation of an

orientation and a habituated monocular color signal, which are used in explaining all other cases throughout this article.

As shown in Figure 19, the two eyes are presented with opposite orientation/color combinations at any given time. During adaptation with C1 stimulus, for example, the left eye is presented with a 135° green grating and the right eye is presented with a 45° magenta grating. The opposite is true for adaptation with a C2 stimulus. When both C1 and C2 adapting stimuli are taken into account together, however, it can be seen that both the left and the right eye are adapted to the same color at any given orientation. For example, the magenta grating is 45° in orientation, whereas the green grating is 135° in orientation. Therefore, 45°-specific feedback pathways to the left and the right LGN learn from habituated magenta activities, and 135°-specific feedback pathways to the left and the right LGN learn from habituated green activities. Thus, tests yield standard aftereffects: tests with a 45° test grating elicit a green aftereffect and tests with a 135° test grating elicit a red aftereffect, even though the two eyes see different orientation/color combinations during adaptation. The McLoughlin model uses a similar mechanism to explain this case because its learning mechanism between the achromatic subsystem and the monocular chromatic subsystem is of the same form as the corticogeniculate feedback learning in the FACADE model.

Previous work on FACADE theory (Grossberg, 1987) has noted how dichoptically presented stimuli whose orientations are perpendicular to each other can give rise to a rivalrous competition between two subpopulations of binocular BCS cells that are tuned to perpendicular orientations. For simplicity, the habituated mechanisms that drive boundary rivalry are not implemented here. In the simulations, this property is implemented by reducing the activities of binocular BCS cells to 75 % of normal activity, but leaving the activities of monocular BCS cells unaffected. This is consistent with the study of Sengpiel *et al.* (1995) who investigated the responses of cat area 17 neurons to study the neural mechanisms responsible for binocular rivalry. By stimulating the two eyes with two gratings oriented perpendicular to each other, they showed that only the binocular neurons were suppressed by the rivalrous stimuli and proposed that the suppressed behavior of the binocular neurons plays a role in binocular rivalry.

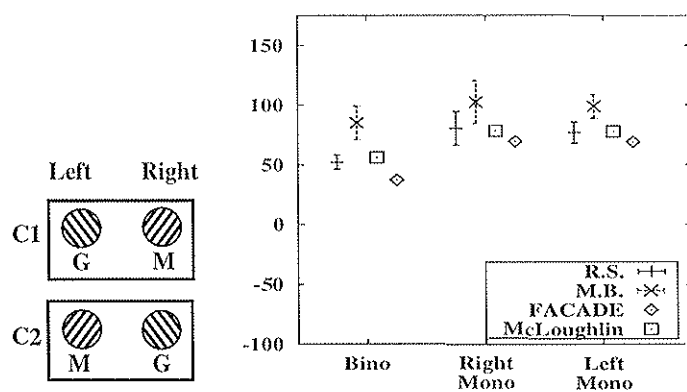


Figure 19: Binocular Rivalry Case: (Left) Adapting stimuli used. (Right) Experimental data and simulation results for the McLoughlin and FACADE models.

## 4 Conclusion

The present article models how the McCollough effect (ME), which is a long-lasting, orientation-contingent complementary color aftereffect, arises. We predict that it occurs as an emergent property when visual learning mechanisms, whose primary role is to adaptively align boundary

and surface representations, interact with habituated transmitter gates in chromatic opponent-processing circuits. Our analysis clarifies why interocular transfer of the ME does not occur under monocular adaptation even though various interocular properties of the ME are known to exist (Vidyasagar, 1976; White *et al.*, 1978), and notably how the Anomalous ME occurs (MacKay & MacKay, 1973). We explained these seemingly conflicting observations by positing multiple learning sites: (1) the pathway connecting the binocular Boundary Contour System (BCS) to the monocular Feature Contour System (FCS); (2) the pathway connecting the monocular FCS to the binocular FCS; and (3) the pathway connecting the binocular BCS to the binocular FCS. In the architecture of the present model, the corticogeniculate feedback pathway was suggested as a possible site to implement the binocular BCS-to-(monocular FCS) pathway. The model, however, could also be interpreted to explain ME data using the pathway from the binocular BCS to the monocular Filling-In Domain, or FIDO. The monocular FIDO is a filling-in stage where featural signals from a single eye are captured in depthful representations by binocular BCS signals. This process has been used to explain data about figure-ground perception and stereopsis (Grossberg, 1994, 1997; Grossberg & McLoughlin, 1997). It was simplified in the present model to become Stage IV in Figure 1. A possible site for the Monocular FIDO *in vivo* is the thin stripes of cortical area V2 (Grossberg, 1997). The model could simulate the present data using such an alternative interpretation because the (binocular BCS)-to-(monocular FIDO) pathway connects the binocular BCS to the monocular FCS, just as the corticogeniculate feedback pathway does.

As described earlier in this article, interocular properties of the ME have not received much theoretical attention. Although there have been two models that describe those properties of the ME (Savoy, 1984; McLoughlin, 1995), they did not offer even a descriptive explanation of the anomalous ME data of MacKay and MacKay (1973), since the color systems in their models were exclusively monocular.

Interocular transfer of the ME does not occur under monocular adaptation in the present model because LGN cells in the unadapted eye are not activated; hence, learning does not occur in the corticogeniculate feedback pathways projecting to the unadapted eye. On the other hand, interocular effects of both orientation and color are observed, even when only partial information about color or orientation is given, in the Anomalous ME Case (a color to one eye, an orientation to the other eye), in the Like Color Case (a color to one eye, an orientation and the same color to the other eye), and in the Different Color Case (a color to one eye, an orientation and the opposite color to the other eye). The model proposes that the binocular cells in the BCS should be "OR" in their nature in order to explain these interocular effects of orientation. This proposal was tested by quantitatively simulating all the experiments using a single set of parameters.

Interocular effects of color were also simulated such that the eye adapted with a homogeneously colored field fails to exhibit the effect in the Different Color Case. The model explains this in terms of the learning in the cortical bottom-up binocular FIDO pathway that competes with the effect of the learning in the corticogeniculate top-down pathway, which would otherwise exhibit a standard ME. Learning in the cortical bottom-up binocular FIDO pathway was also used in the Anomalous ME Case to explain how the eye adapted with an achromatic grating exhibits a chromatic aftereffect of the *same* color to the adapting color of the other eye.

In the present article, we have focused on how adaptive mechanisms in the nervous system generate changes in neural loci that subserve the ME as their perceptual outcome. There have been several other theoretical attempts to do this. Some of them suggested that the ME arises from the fatigue of neurons that are tuned to both orientation and color (McCollough, 1965; Stromeyer & Dawson, 1978; Michael, 1978). Some "double-duty" neurons that are tuned to both orientation and color are, indeed, found in monkey visual cortex (Michael, 1978). These proposals, however, do not seem to be adequate because: (1) Fatigue alone cannot explain the persistence of the ME over time; and (2) these cells cannot subserve the interocular effects of the ME since they are

monocular cells (Michael, 1978). Others have suggested that the persistence of the ME arises from synaptic changes in the connection between neurons for orientation and neurons for color (Murch & Hirsch, 1972; Savoy, 1984; McLoughlin, 1995). These models, including the McLoughlin model, were also incomplete, however, because they were not able to explain the anomalous ME data of MacKay and MacKay (1973), where there was interocular effects of color information. Also these models did not give a functional rationale for why such adaptive pathways are needed during normal vision.

Another class of theories does focus on the functional importance of the ME. In some of these theories, the ME is proposed to arise from a process of correcting errors and biases that are imposed during adaptations in ME experiments. For example, Shute (1979) suggested that the spurious correlations between pattern and color induced by adapting gratings are recorded in the hippocampus. When the pattern is subsequently presented alone during test trials, an inhibitory mechanism in the hippocampus was proposed to inhibit neurons for the adapting color and to disinhibit neurons for the opponent color, resulting in the perception of a complementary color. Evidence for such a hippocampal process seems to be lacking, including evidence for cells with these featural properties.

Dodwell and Humphrey (1990) proposed that the presentation of, say, a red vertical adapting grating will shift the "neutral point" for red-vertical correlations toward the red side of the color continuum. The shift occurs because a hypothesized mechanism, called an "error correcting device", is at work in order to maintain a color-pattern neutrality. After the shift, an achromatic vertical test grating would appear greenish because an achromatic light, which was previously a neutral point, now lie on the green side of the shifted color continuum. A similar argument is found in the Warren (1985) proposal of a "criterion shift rule". Bedford and colleagues (Bedford & Reinke, 1993; Bedford, 1995) also suggested that the ME arises in order to correct a perceptual error that arises when there is a violation of a perceptual constraint that an object should not change its color when it is rotated, since the presentation of a pair of adapting gratings of opposite color and orientation can be interpreted as a change of color of a single object that is rotated 90°. Our own explanation of these data employs mechanisms that operate at lower cortical levels than those involved in invariant pattern recognition.

In other functional theories (Hohmann & von der Malsburg, 1978; Held, 1980; Broerse *et al.*, 1999), the ME was proposed to arise from neural processes whose normal function is to compensate for chromatic aberration of the eye (Hay *et al.*, 1963), which are revealed in experiments where subjects wear prism goggles that differentially bend lights of different wavelengths (Kohler, 1962; Harris, 1980). This type of theory is of particular interest concerning the lack of interocular transfer in the ME because it makes intuitive sense for the compensation processes for chromatic aberrations not be transferred interocularly because the two eyes differ in their aberrations (Held, 1980).

Our strong advantage of the present model, apart from the ME data-prediction properties, is that its main concepts and mechanisms were not derived to explain ME data. Rather, they are natural consequences of the FACADE theory prediction that boundaries and surfaces are computed by parallel cortical processing streams, a hypothesis for which there is now a lot of experimental evidence; e.g., Dresp and Grossberg (1997, 1999), Elder and Zucker (1998), Lamme *et al.* (1999), Rogers-Ramachandran and Ramachandran (1998).

Although not simulated here, several other known properties of the ME can also be explained by the present model. It has been shown that the ME can be induced not only by scanning the adapting patterns, but also by fixating them. The induction of the ME during fixation is selective to retinotopy, such that the aftereffect is seen only when the test gratings fall on the same retinal position as the adapting gratings (Stromeyer & Dawson, 1978). The present model can explain the scanning case since adaptive pathways across the visual field adapt equally on the average

during scanning. The fixation case can also be explained, since only the pathways whose retinal locations of receptive fields lie within the colored stripes of adapting gratings can adapt. Extinction properties of the ME, which show that the ME decays faster due to viewing of achromatic gratings (Skowbo *et al.*, 1974), can also be explained by the present model. Since achromatic gratings equally activate both the magenta and green LGN cells, any imbalance that was caused by prior color adaptation disappears. The observation that monocular viewing of achromatic gratings does not extinguish a binocularly induced ME of the other eye (Savoy, 1984) is also explained by the model because the achromatic gratings seen in the one eye removes the imbalance caused by prior color adaptation only in that eye, but not in the other eye.

Additional support for the present model comes from the Meyer and Dougherty (1987) study on how the ME depends on boundary salience. In that study, the test pattern was a subjective contour version of a faces-and-vase figure, where the faces and vase part of the figure was made of vertical and horizontal gratings, respectively, in order to induce an illusory boundary between faces and vase. The figure can be perceived as two faces consisting of vertical gratings, a vase consisting of horizontal gratings, or concentric squares consisting of both vertical and horizontal gratings. After adaptation to colored vertical and horizontal gratings, subjects reported the ME when the figure was perceived as two faces or a vase but not with the perception of concentric squares. As the authors pointed out, the ME can be observed only with the perception of two faces or a vase because filling-in of the ME hue stops at the subjective contour established by the BCS. The ME cannot be observed with the perception of concentric squares because the opposite ME hues elicited by vertical and horizontal gratings in the test figure fill-in throughout the square and thus cancel out with each other due to the lack of subjective contour. Similarly, Broerse and O'Shea (1995) and Broerse *et al.* (1999) conjectured that the ME involves a filling-in process of the type used by the FACADE model, using the two proposed components of the ME: edge colors located at edges of contours, and spread colors that spread away from edge colors in order to fill-in adjacent white stripes of test patterns.

In summary, the present article extends the explanatory range of FACADE theory to explain the ME, particularly data concerning how interocular properties of the ME arise. The model explains them as perceptual consequences of the visual system mechanisms whose primary role is to establish and maintain a topographic mapping between boundary and surface representations, which compensates for the positional displacement that occurs in the boundary system due to binocular fusion and allelotropia.

## APPENDIX: Equations and Parameters

The one-dimensional simulations use an array of 300 units. Unless otherwise stated, differential equations were solved numerically by Euler's method with step size 0.2. Computations were done in C programming language with a GNU C compiler on an IBM-compatible PC with a LINUX operating system.

### Retina and LGN cells (Figure 1, Stage I and Stage II)

Three types of wavelength-sensitive inputs are modeled at each position  $i$ : achromatic ( $a_i$ ), magenta ( $m_i$ ), and green ( $g_i$ ). They are combined as follows to form inputs to the model LGN cells:

$$I_i^a = a_i \quad (1)$$

$$I_i^m = m_i + \rho a_i \quad (2)$$

and

$$I_i^g = g_i + \rho a_i, \quad (3)$$

where  $I_i^a$  denotes input to achromatic LGN cells,  $I_i^m$  denotes input to magenta LGN cells, and  $I_i^g$  denotes input to green LGN cells. Equations (2) and (3) say that the achromatic input not only activates achromatic LGN cells, but also chromatic LGN cells. This indirect activation of chromatic cells by an achromatic test input is one basis of the ME. Parameter  $\rho$  specifies the relative sizes of chromatic and achromatic inputs. For simplicity of notation, Equations (2) and (3) can be expressed in a single equation as:

$$I_i^{m/g} = (m_i/g_i) + \rho a_i. \quad (4)$$

This type of notation with slash (/) to mean "either or" will be used throughout this paper whenever needed.

Grating inputs are represented as interdigitating one black stripe and two colored stripes of an amplitude of 10.0, presented in a black background. A magenta grating input, for example, is represented as  $I_i^m = 10.0$  for  $75 \leq i < 125$  and for  $175 \leq i < 225$ , and  $I_i^m = 0.0$  for all other  $i$ . A homogeneous magenta field, for example, is represented as  $I_i^m = 10.0$  for  $75 \leq i < 225$ , and  $I_i^m = 0.0$  for all other  $i$ .

Since there are two eyes in the system, a general form of LGN input for a given eye and color can be represented as  $I_i^{ec}$ , where the superscript  $e$  (eye) is either  $l$  (left) or  $r$  (right), and the superscript  $c$  (color) is either  $a$  (achromatic),  $m$  (magenta), or  $g$  (green). Hence, chromatic LGN inputs to the left eye, for example, can be expressed as:

$$I_i^{l(m/g)} = (m_i^l/g_i^l) + \rho a_i^l. \quad (5)$$

The activity  $s_i$  of the LGN cell at position  $i$  obeys a membrane equation:

$$\frac{d}{dt}s_i = -A_1 s_i + (B_1 - s_i) \sum_{k=1}^N I_k C_{1ki} - (s_i + D_1) \sum_{k=1}^N I_k E_{1ki}, \quad (6)$$

where  $N$  is the number of cells in the system, and the terms  $\sum_{k=1}^N I_k C_{1ki}$  and  $\sum_{k=1}^N I_k E_{1ki}$  represent on-center and off-surround inputs, respectively (Grossberg, 1973, 1983). Excitatory ( $C_{1ki}$ ) and inhibitory ( $E_{1ki}$ ) on-center and off-surround receptive fields, respectively, are defined by Gaussian kernels:

$$C_{1ki} = C_1 \exp \left[ -\frac{1}{\theta_1^2} (k - i)^2 \log 2 \right] \quad (7)$$

and

$$E_{1ki} = E_1 \exp \left[ -\frac{1}{\lambda_1^2} (k - i)^2 \log 2 \right]. \quad (8)$$

In the simulations, Equation (6) is solved at equilibrium so that:

$$s_i = \frac{\sum_{k=1}^N (B_1 C_{1ki} - D_1 E_{1ki}) I_k}{A_1 + \sum_{k=1}^N (C_{1ki} + E_{1ki}) I_k}. \quad (9)$$

The output signal from each LGN cell is half-wave rectified:

$$S_i = [s_i]^+, \quad (10)$$

with  $[x]^+ = \max(x, 0)$ . As described previously, activities of LGN cells for a given ocularity and color can be obtained by putting appropriate superscripts in Equation (9).

### Monocular transmitter habituation (Figure 1, Pathway 2)

The transmitter level  $t_i$  of the  $i$ th LGN cell pathway is described by the following transmitter habituation, or depression equation (Abbott *et al.*, 1997; Francis *et al.*, 1994; Francis & Grossberg, 1996; Grossberg, 1968, 1969):

$$\frac{d}{dt} t_i = \eta_1 [L_1 - (1 + \mu_1 S_i) t_i]. \quad (11)$$

In Equation (11), transmitter accumulates to target level  $L_1$  at rate  $\eta_1$  via term  $\eta_1 (L_1 - t_i)$ , and is inactivated, or released, in an activity-dependent way at rate  $-\eta_1 \mu_1 S_i t_i$ . Transmitter output is proportional to its inactivation rate:

$$T_i = S_i t_i. \quad (12)$$

The same Equations (11) and (12) exist for each ocularity and color.

### BCS cells (Figure 1, Stage V)

BCS cells detect boundary structures in the stimulus. BCS cells are tuned to orientation and ocularity. In the simulations, two orientations ( $45^\circ$  and  $135^\circ$ ) and three ocularities (left monocular, binocular, and right monocular) are considered. The orientational preference is assumed to be exclusive such that there exists two separate pools of cells that are tuned to the orientation of  $45^\circ$  or  $135^\circ$ . The ocularity preference, however, is assumed to be non-exclusive such that binocular BCS cells respond not only to binocular stimulation but also to monocular stimulation, although they respond more strongly to the former than the latter. Similarly, monocular BCS cells prefer monocular stimulation but also respond to binocular stimulation to some extent. Therefore, the following four constants describe BCS cell activities:  $B_B$  denotes binocular cell activity under binocular stimulation,  $B_M$  denotes binocular cell activity under monocular stimulation,  $M_M$  denotes monocular cell activity under monocular stimulation, and  $M_B$  denotes monocular cell activity under binocular stimulation.

Activities of BCS cells at position  $j$  are denoted as  $A_j$ . For simplicity, only those BCS cells located at the positions corresponding to edges of input stimuli are activated to one of the four values. For example, when the network is presented with binocular gratings whose edge locations of stripes are  $i = 75, 125, 175, 225$ , BCS cells become activated such that  $A_j = B_B$  for  $j = 75, 125, 175, 225$ , and  $A_j = 0$  for all other  $j$ .

Since BCS cells are tuned to orientation and ocularity, BCS cell activities can be denoted as  $A_j^{od}$  where the superscript  $o$  (ocularity) denotes ocularity (which is either  $l$  for monocular left,  $r$  for monocular right, or  $b$  for binocular) and  $d$  (degree) denotes orientation (which is either  $45^\circ$  or  $135^\circ$ ).

### Cortico-geniculate feedback pathway (Figure 1, Pathway 3)

The adaptive weight in the feedback pathways from the  $j^{\text{th}}$  V1 cell to the  $i^{\text{th}}$  LGN cell is denoted by  $z_{ji}$ , and the long-term change of synaptic efficacy in this pathway is described by:

$$\frac{d}{dt}z_{ji} = \gamma_1 A_j T_i (-z_{ji} + \kappa_1 T_i). \quad (13)$$

In Equation (13),  $T_i$  is the habituating output of the  $i^{\text{th}}$  LGN cell, as in Equation (12). The output is assumed to be proportional to the activity of the LGN cell that  $z_{ji}$  samples; see Figure 1. Term  $A_j T_i$  in Equation (13) states that adaptive weight of the top-down pathway is modified only when both pre- and postsynaptic cells are active. Term  $-z_{ji} + \kappa_1 T_i$  says that the weight decreases when the post-synaptic activity  $T_i$  habituates.

Since BCS cells are tuned to ocularity and orientation and LGN cells to ocularity and color, the feedback pathway between them can be labeled by a set of four superscripts;  $o$  (ocularity),  $d$  (degree),  $e$  (eye), and  $c$  (color). For example, the pathway from the binocular BCS cell ( $b$ ) with  $45^\circ$  orientational preference ( $45$ ) to the left ( $l$ ) magenta ( $m$ ) LGN cell can be denoted as  $z_{ji}^{b45lm}$ . In this way, each pathway can be expressed as Equation (13) with an appropriate use of superscripts.

Initially, all feedback weights start out small and equal ( $z_{ji} = 0.0001$  for all  $j, i$ ). Feedback weights then self-organize according to Equation (13) in response to gratings whose amplitude and pattern are the same as the gratings used in ME adaptations. The purpose of self-organization is to obtain the values of weights that the system would have under normal conditions (that is, prior to ME adaptations). Therefore, the self-organization employs binocular gratings and no transmitter habituation because humans usually view the world binocularly and do not usually stare at objects long enough to cause major amounts of transmitter habituation, as described earlier. The values of the self-organized weights are the initial values with which ME adaptation and learning take place.

The feedback pathway also acts as a gating signal for LGN output signals (Gove *et al.*, 1995; Pollen, 1999; Sillito *et al.*, 1994). Hence, the bottom-up LGN output signals under the influence of feedback matching and selection,  $r_i$  are described by:

$$r_i = \sum_o \sum_d \sum_j A_j^{od} z_{ji}^{odec} T_i^{ec}. \quad (14)$$

Equation (14) states that the feedback ( $A_j z_{ji}$ ) modulates bottom-up output signals by a top-down multiplicative gating process of the LGN activity ( $T_i$ ), summed over all ocularity ( $o$ ) and orientation ( $d$ ) of cortical BCS cells.

According to equation (14), the LGN output  $r_i$  will be zero if all the feedback gating signals  $A_j$  are zero. This might seem to imply that bottom-up signals from the LGN could never activate higher processing stages, including the boundaries that activate the terms  $A_j$ , since the boundary terms  $A_j$  would have zero activity unless they were first activated by bottom-up inputs, such as  $r_i$ . A more general expression, which replaces  $A_j$  by a constant bottom-up gain plus the top-down gain  $A_j$ , would overcome this problem. The constant bottom-up gain would enable bottom-up signals  $r_i$  to activate higher processing stages. Once activated, the top-down gain would then multiplicatively enhance bottom-up processing. Neurophysiological data concerning the effects of cortico-geniculate feedback support the idea that such a multiplicative top-down effect exists

(Przybylski *et al.*, 2000; Sillito *et al.*, 1994). A top-down multiplicative gain has also been used in neural models that simulate data about corticogeniculate feedback (e.g., Gove *et al.* (1995)). In the present model, the top-down terms  $A_j$  were chosen algorithmically to be constants, The present formulation with terms  $A_j$  alone is thus equivalent to a formulation with  $A_j$  plus a constant bottom-up gain, with a suitable change in the numerical values of  $A_j$ , since the simulations consider only times when both bottom-up and top-down processes are already active, and focus on more slowly varying processes like habituation and learning.

The bottom-up output signals are opponently processed between magenta and green cells before they activate cortical cells and initiate filling-in:

$$R_i^{m/g} = \left[ r_i^{m/g} - r_i^{g/m} \right]^+ . \quad (15)$$

### Binocular summation

Opponent processed monocular FCS activities are transmitted to the binocular summation stage by the cortical bottom-up binocular FIDO pathway. The net transmitted signal,  $y_i$ , to the  $i^{\text{th}}$  binocular FIDO cell is given by:

$$y_i = R_i Z_i, \quad (16)$$

where  $Z_i$  is the bottom-up adaptive weight in this pathway. The monocular inputs from the left and the right eyes are binocularly summed, as in Grossberg and Kelly (1999), by the following membrane equation:

$$\frac{d}{dt} s_i^b = -A_2 s_i^b + (B_2 - s_i^b) \sum_{k=1}^N C_{2ki} \left[ f(y_k^l) + f(y_k^r) \right] - (s_i^b + D_2) \sum_{k=1}^N E_{2ki} \left[ g(y_k^l) + g(y_k^r) \right], \quad (17)$$

where excitatory ( $C_{2ki}$ ) and inhibitory ( $E_{2ki}$ ) kernels are defined in the same manner as in Equation (7) and (8). Excitatory and inhibitory signal functions  $f(x)$  and  $g(x)$ , respectively, are defined as:

$$f(x) = \frac{[x - \Gamma]^{+2}}{\alpha^2 + [x - \Gamma]^{+2}} \quad (18)$$

and

$$g(x) = \frac{[x - \Gamma]^+}{\alpha + [x - \Gamma]^+}. \quad (19)$$

See Grossberg and Kelly (1999) for how these signal functions helps to quantitatively simulate binocular brightness data. In the simulations, Equation (17) for the activity  $s_i^b$  of the  $i^{\text{th}}$  binocular FIDO cell is solved at equilibrium. The output signals from the binocular FIDO are half-wave rectified:

$$S_i^b = \left[ s_i^b \right]^+ . \quad (20)$$

### Binocular transmitter habituation

As in Equations (11) and (12), the transmitter levels at the binocular summation stage,  $t_i^b$ , are described by the equation:

$$\frac{d}{dt} t_i^b = \eta_2 \left[ L_2 - \left( 1 + \mu_2 S_i^b \right) t_i^b \right]. \quad (21)$$

Transmitter-gated output obeys:

$$T_i^b = S_i^b t_i^b. \quad (22)$$

Transmitter-gated outputs are then opponently processed between magenta and green cells:

$$O_i^{b,(m/g)} = \left[ T_i^{b,(m/g)} - T_i^{b,(g/m)} \right]^+ . \quad (23)$$

## Cortical bottom-up FCS pathway (Figure 1, Pathway 6)

The long-term changes in the synaptic efficacy of the cortical bottom-up binocular FIDO pathway are described by:

$$\frac{d}{dt}Z_i = \gamma_2 R_i O_i^b (-Z_i + \kappa_2 O_i^b). \quad (24)$$

Hence, the cortical bottom-up learning described by Equation (24) is of the same form as the top-down learning described previously by Equation (13). This learning helps to binocularly align monocular featural signals that correspond to the same object features. Since the cortical bottom-up FCS pathways connect monocular-color surfaces with binocular-color surfaces, a superscript is needed to denote each specific pathway. For example, the pathway from a monocular green cell to a binocular magenta cell is denoted as  $Z_i^{gm}$ .

Initially, all cortical bottom-up weights start out small and equal ( $Z_i = 0.03$  for all  $i$ ). Bottom-up weights then self-organize according to Equation (24) in the same manner as previously described for corticogeniculate feedback weights. The values of the self-organized weights are the initial values with which ME adaptation and learning take place.

## Binocular FIDO and binocular boundary

Binocularly summated featural properties, such as color, generate a visible surface representation at the final level of the FCS, which is called *Binocular Filling-In Domain* (FIDO). The binocular FIDO (Figure 1, Stage VI) contains an array of intimately connected cells such that neighboring cells can rapidly spread activities between each other's compartment membranes via a process of diffusion.

The diffusive spreading, or filling-in, of activation in the binocular FIDO is restricted to the compartments that are formed by binocular boundaries, which act as barriers to filling-in. The diffusion coefficients that restrict the magnitude of cross influence of location  $i$  with location  $k$  decrease as the binocular boundary signals  $B_{ji}$  and  $B_{jk}$  increase:

$$P_{ki} = \frac{\delta}{\beta + \nu \sum_o \sum_d \sum_j A_j^{od} (B_{jk}^{od} + B_{ji}^{od})}. \quad (25)$$

Binocular boundary learning is described by:

$$\frac{d}{dt}B_{ji} = \gamma_3 A_j o_i^b (-B_{ji} + \kappa_3 o_i^b), \quad (26)$$

where  $o_i^b$  is computed by sharpening binocular FCS activity  $O_i^b$  by raising it to the  $n$ th power and normalizing it:

$$o_i^b = \left[ \frac{(O_i^b)^n}{\left[ \omega^n + \sum_{k=1}^N (C_{3ki} O_k)^n \right]} - \Omega \right]^+. \quad (27)$$

The operation in Equation (27) sharpens spatial patterns in the FCS so that spatially-localized boundary structures corresponding to the FCS patterns are formed, while ensuring analog-sensitivity of the boundary values (i.e., large amplitudes of FCS signals result in large amplitudes of boundary signals).

The binocular boundary learning described by Equation (26) is of the same form as Equation (13) and (24). It is one of the learning processes that align boundary and surface representations.

As with corticogeniculate feedback weights and cortical bottom-up weights, the BCS boundary strengths initially start out small and equal ( $B_{ji} = 0.00001$  for all  $j, i$ ) and then self-organize for 50 iterations of numerical integrations, as described previously.

Each activity  $x_i$  at position  $i$  of the binocular FIDO uses a nonlinear diffusion equation to fill-in surface color (Grossberg & Todorović, 1988):

$$\frac{d}{dt}x_i = -x_i + \sum_{k \in N_i} (x_k - x_i)P_{ki} + O_i^b. \quad (28)$$

The adaptively aligned boundaries in Equation (26) determine the permeabilities  $P_{ki}$ , which are defined by Equation (25), and the set  $N_i$  of locations contains only the nearest neighbors of  $i$ :

$$N_i = (i - 1), (i + 1). \quad (29)$$

According to Equation (28), each potential  $x_i$  is activated by  $O_i^b$  and thereupon engages in passive decay (term  $-x_i$ ) and diffusive filling-in with its two nearest neighbors to the degree permitted by the diffusion coefficient  $P_{ki}$ . Opponent processing of the binocular FIDO activities gives the final perceptual activity:

$$X_i^{m/g} = [x_i^{m/g} - x_i^{g/m}]^+. \quad (30)$$

The filled-in value corresponding to the middle spatial position in the white stripe regions is compared to the experimental data, which describe the relative strengths of aftereffects. The filled-in value obtained from the binocular test of the Standard Binocular Case is used to normalize all other results. These normalized results represent relative strengths of the ME and are used to fit the data in all thirteen experiments.

## Parameters

In all simulations, the following parameter values are used. Among these parameters, the parameters for BCS cell activities ( $B_B, B_M, M_M, M_B$ ) have been thoroughly analyzed in the simulations to fit the experimental data, as described earlier in this article.

### Retina and LGN cells

$$N = 300, \rho = 0.5, A_1 = 1.0, B_1 = 9.0, C_1 = 4.0, D_1 = 5.0, E_1 = 0.4, \theta_1 = 1.0, \lambda_1 = 8.0.$$

### Monocular transmitter habituation

$$\eta_1 = 0.5, L_1 = 1.0, \mu_1 \text{ for chromatic cell} = 1.0, \mu_1 \text{ for achromatic cell} = 0.05.$$

### BCS cells

$$B_B = 0.30, M_M = 0.44, B_M = 0.23, M_B = 0.21.$$

### Corticogeniculate feedback pathway

$$\gamma_1 = 0.1, \kappa_1 = 1.0.$$

### Binocular summation

$$A_2 = 10.0, B_2 = 5.0, C_2 = 4.0, D_2 = 1.0, E_2 = 0.4, \theta_2 = 1.0, \lambda_2 = 8.0, \alpha = 3.0, \Gamma = 0.0.$$

### Binocular transmitter habituation

$$\eta_2 = 0.1, L_1 = 1.0, \mu_2 = 0.1.$$

### Cortical bottom-up FCS pathway

$$\kappa_2 = 0.5, \gamma_2 \text{ for same color association} = 0.2, \gamma_2 \text{ for achromatic-to-chromatic association} = 0.002, \gamma_2 \text{ for different color association} = 0.0005.$$

### Binocular FIDO and binocular boundary

$$\delta = 1000.0, \beta = 0.01, \nu = 30.0, \gamma_3 = 1.0, \kappa_3 = 10.0, \omega = 0.70, C_3 = 1.0, \theta_3 = 20.0, n = 50.0, \Omega = 0.24.$$

## References

- Abbott, L. F., Varela, J. A., Sen, K., & Nelson, S. B. (1997). Synaptic depression and cortical gain control. *Science*, *275*, 220–223.
- Allan, L. G., & Siegel, S. (1997). Contingent color aftereffects: reassessing old conclusions. *Perception & Psychophysics*, *59*(1), 129–141.
- Baloch, A. A., Grossberg, S., Mingolla, E., & Nogueira, C. A. (1999). Neural model of first-order and second-order motion perception and magnocellular dynamics. *Journal of the Optical Society of America, A*, *16*(5), 953–978.
- Bedford, F. L. (1995). Constraints on perceptual learning: objects and dimensions. *Cognition*, *54*, 253–297.
- Bedford, F. L., & Reinke, K. S. (1993). The McCollough effect: dissociating retinal from spatial coordinates. *Perception & Psychophysics*, *54*(4), 515–526.
- Broerse, J., & O'Shea, R. P. (1995). Local and global factors in spatially-contingent coloured after-effects. *Vision Research*, *35*(2), 207–226.
- Broerse, J., Vladusich, T., & O'Shea, R. (1999). Colour at edges and colour spreading in McCollough effects. *Vision Research*, *39*, 1305–1320.
- Carpenter, G. A., & Grossberg, S. (1981). Adaptation and transmitter gating in vertebrate photoreceptors. *Journal of Theoretical Neurobiology*, *1*, 1–42. Reprinted in: Grossberg, S. (1987). *The adaptive brain: II. Vision, speech, language, and motor control*. Amsterdam: North-Holland.
- Cohn, T. E., & Lasley, D. J. (1986). Visual sensitivity. *Annual Reviews Psychology*, *37*, 495–521.
- Dodwell, P. C., & Humphrey, G. K. (1990). A functional theory of the McCollough effect. *Psychological Review*, *97*(1), 78–89.
- Dresp, B., & Grossberg, S. (1997). Contour integration across polarities and spatial gaps: from local contrast filtering to global grouping. *Vision Research*, *37*(7), 913–924.
- Dresp, B., & Grossberg, S. (1999). Spatial facilitation by color and luminance edges: boundary, surface, and attentional factors. *Vision Research*, *39*, 3431–3443.
- Elder, J. H., & Zucker, S. W. (1998). Evidence for boundary-specific grouping. *Vision Research*, *328*, 143–152.
- Francis, G., & Grossberg, S. (1996). Cortical dynamics of boundary segmentation and reset: persistence, afterimages, and residual traces. *Perception*, *25*, 543–567.
- Francis, G., Grossberg, S., & Mingolla, E. (1994). Cortical dynamics of feature binding and reset: control of visual persistence. *Vision Research*, *34*(8), 1089–1104.
- Gove, A., Grossberg, S., & Mingolla, E. (1995). Brightness preception, illusory contours, and corticogeniculate feedback. *Visual Neuroscience*, *12*, 1027–1052.
- Grieve, K. L., & Sillito, A. M. (1995). Differential properties of cells in the feline primary visual cortex providing the corticofugal feedback to the lateral geniculate nucleus and visual claustrum. *The Journal of Neuroscience*, *15*(7), 4868–4874.

- Grossberg, S. (1968). Some physiological and biochemical consequences of psychological postulates. *Proceedings of the National Academy of Sciences*, 60, 758–765.
- Grossberg, S. (1969). On the production and release of chemical transmitters and related topics in cellular control. *Journal of Theoretical Biology*, 22, 325–364.
- Grossberg, S. (1973). Contour enhancement, short-term memory and constancies in reverberating neural networks. *Studies in Applied Mathematics*, 52, 217–257.
- Grossberg, S. (1980). How does a brain build a cognitive code?. *Psychological Review*, 87, 1–51.
- Grossberg, S. (1983). The quantized geometry of visual space: The coherent computation of depth, form, and lightness. *Behavioral and Brain Sciences*, 6, 625–657.
- Grossberg, S. (1987). Cortical dynamics of three-dimensional form, color, and brightness perception: II. Binocular theory. *Perception & Psychophysics*, 41(2), 117–158.
- Grossberg, S. (1994). 3-D vision and figure-ground separation by visual cortex. *Perception & Psychophysics*, 55(1), 48–120.
- Grossberg, S. (1997). Cortical dynamics of three-dimensional figure-ground perception of two-dimensional pictures. *Psychological Review*, 104(3), 618–658.
- Grossberg, S., & Kelly, F. (1999). Neural dynamics of binocular brightness perception. *Vision Research*, 39(22), 3796–3816.
- Grossberg, S., & McLoughlin, N. P. (1997). Cortical dynamics of three-dimensional surface perception: binocular and half-occluded scenic images. *Neural Networks*, 10(9), 1583–1605.
- Grossberg, S., Mingolla, E., & Ross, W. (1997). Visual brain and visual perception: how does the cortex do perceptual grouping?. *Trends in Neurosciences*, 20(3), 106–111.
- Grossberg, S., & Pessoa, L. (1998). Texture segregation, surface representation and figure-ground separation. *Vision Research*, 38, 2657–2684.
- Grossberg, S., & Todorović, D. (1988). Neural dynamics of 1-D and 2-D brightness perception: a unified model of classical and recent phenomena. *Perception & Psychophysics*, 43, 241–277.
- Grunewald, A., & Grossberg, S. (1998). Self-organization of binocular disparity tuning by reciprocal corticogeniculate interactions. *Journal of Cognitive Neuroscience*, 10(2), 199–215.
- Harris, C. S. (1980). Insight or out of sight?: two examples of perceptual plasticity in the human adult. In Harris, C. S. (Ed.), *Visual coding and adaptability*. New Jersey: Hillsdale.
- Hay, J. C., Pick, Jr., H. L., & Rosser, E. (1963). Adaptation to chromatic aberration by the human visual system. *Science*, 141, 167–169.
- Held, R. (1980). The rediscovery of adaptability in the visual system: effects of extrinsic and intrinsic chromatic dispersion. In Harris, C. S. (Ed.), *Visual coding and adaptability*. New Jersey: Hillsdale.
- Hohmann, A., & von der Malsburg, C. (1978). McCollough effect and eye optics. *Perception*, 7, 551–555.
- Hubel, D. H., & Wiesel, T. N. (1962). Receptive fields, binocular interaction and functional architecture in the cat's visual cortex. *Journal of Neurophysiology*, 160, 106–154.

- Kato, H., Bishop, P. O., & Orban, G. A. (1981). Binocular interaction on monocularly discharged lateral geniculate and striate neurons in the cat. *Journal of Neurophysiology*, 46(5), 932–951.
- Kelly, F., & Grossberg, S. (1998). Neural dynamics of 3-D surface perception: Figure-ground separation and lightness perception. Tech. rep. CAS/CNS TR-98-026, Boston University.
- Kohler, I. (1962). Experiments with goggles. *Scientific American*, 206, 62–72.
- Krüger, J. (1979). McCollough effect: a theory based on the anatomy of the lateral geniculate body. *Perception & Psychophysics*, 25(3), 169–179.
- Lamme, V. A., Rodriguez-Rodriguez, V., & Spekreijse, H. (1999). Separate processing dynamics for texture elements, boundaries and surfaces in primary visual cortex of the macaque monkey. *Cerebral Cortex*, 9, 406–413.
- Lehmkuhle, S. M., & Fox, R. (1976). On measuring interocular transfer. *Vision Research*, 16, 428–430.
- MacKay, D. M., & MacKay, V. (1973). Orientation-sensitive after-effects of dichoptically presented colour and form. *Nature*, 242, 477–479.
- McCollough, C. (1965). Color adaptation of edge-detectors in the human visual system. *Science*, 149, 1115–1116.
- McLoughlin, N. P. (1995). *Neural network models of 3-D surface perception: Da Vinci stereopsis and the McCollough effect*. Ph.D. thesis, Boston University.
- Meyer, G. E., & Dougherty, T. (1987). Effects of flicker-induced depth on chromatic subjective contours. *Journal of Experimental Psychology: Human Perception and Performance*, 13(3), 353–360.
- Michael, C. R. (1978). Color vision mechanisms in monkey striate cortex: simple cells with dual opponent-color receptive fields. *Journal of Neurophysiology*, 41(5), 1233–1249.
- Murch, G. M. (1976). Classical conditioning of the McCollough effect: temporal parameters. *Vision Research*, 16, 615–619.
- Murch, G. M., & Hirsch, J. (1972). The McCollough effect created by complementary afterimages. *American Journal of Psychology*, 85(2), 241–247.
- Murphy, P. C., Duckett, S. G., & Sillito, A. M. (1999). Feedback connection to the lateral geniculate nucleus and cortical response properties. *Science*, 286, 1552–1554.
- Ögmen, H., & Gagne, S. (1990). Neural models of SUSTAINED and ON-OFF units of insect lamina. *Biological Cybernetics*, 63(1), 51–60.
- Pettigrew, J. D., Nikara, T., & Bishop, P. O. (1968). Binocular interaction on single units in cat striate cortex: simultaneous stimulation by single moving slit with receptive fields in correspondence. *Experimental Brain Research*, 6, 391–410.
- Pollen, D. A. (1999). On the neural correlates of visual perception. *Cerebral Cortex*, 9, 4–19.
- Przybylski, A. W., Gaska, J. P., Foote, W., & Pollen, D. A. (2000). Striate cortex increases contrast gain of macaque LGN neurons. *Visual Neuroscience*, 17, 485–494.
- Rogers-Ramachandran, D. C., & Ramachandran, V. S. (1998). Psychophysical evidence for boundary and surface systems in human vision. *Vision Research*, 38, 71–77.

- Savoy, R. L. (1984). "Extinction" of the McCollough effect does not transfer interocularly. *Perception & Psychophysics*, 36(6), 571–576.
- Sengpiel, F., Blakemore, C., & Harrad, R. (1995). Interocular suppression in the primary visual cortex: a possible neural basis of binocular rivalry. *Vision Research*, 35(2), 179–195.
- Shute, C. C. D. (1979). *The McCollough effect: an indicator of central neurotransmitter activity*. Cambridge: Cambridge University Press.
- Sillito, A. M., Jones, H. E., Gerstein, G. L., & West, D. C. (1994). Feature-linked synchronization of thalamic relay cell firing induced by feedback from the visual cortex. *Nature*, 369(9), 479–482.
- Skowbo, D., Gentry, T., Timney, B., & Morant, R. (1974). The McCollough effects: Influence of several kinds of visual stimulation on decay rate. *Perception & Psychophysics*, 16, 47–49.
- Skowbo, D., & White, K. (1983). McCollough effect acquisition depends on duration of exposure to inducing stimuli, not number of stimulus presentation. *Perception & Psychophysics*, 34, 549–551.
- Stromeyer, C. F., & Dawson, B. M. (1978). Form-colour aftereffects: selectivity to local luminance contrast. *Perception*, 7, 407–415.
- Vidyasagar, T. R. (1976). Orientation specific colour adaptation at a binocular site. *Nature*, 261, 39–40.
- von Tschermak-Seysenegg, A. (1952). *Introduction to physiological optics* (P. Boeder, Trans.). Springfield, IL: Thomas.
- Warren, R. M. (1985). Criterion shift rule and perceptual homeostasis. *Psychological Review*, 92(4), 574–584.
- Watanabe, T., Zimmerman, G. L., & Cavanagh, P. (1992). Orientation-contingent color aftereffects mediated by subjective transparent structures. *Perception & Psychophysics*, 52(2), 161–166.
- Werner, H. (1937). Dynamics in binocular depth perception. *Psychological Monograph*, 218.
- White, K. D., Petry, H. M., Riggs, L. A., & Miller, J. (1978). Binocular interactions during establishment of McCollough effects. *Vision Research*, 18, 1201–1215.